INVESTIGATING NOVEL β-CATENIN SIGNALLING MECHANISMS IN AN EMBRYONIC STEM CELL MODEL

INVESTIGATING NOVEL β-CATENIN SIGNALLING MECHANISMS IN AN EMBRYONIC STEM CELL MODEL

BY

SOLEN ABDULLA, B.Sc. (Honours)

A Thesis

Submitted to the School of Graduate Studies

In Partial Fulfillment of the Requirements

For the Degree

Master of Science

McMaster University

Descriptive Note

MASTER OF SCIENCE (2017)	McMaster University
(Biochemistry)	Hamilton, Ontario
TITLE:	Investigating Novel β-catenin Signalling Mechanisms in an Embryonic Stem Cell Model
AUTHOR:	Solen Abdulla, B.Sc. (Honours)
SUPERVISOR:	Dr. Bradley Doble
NUMBER OF PAGES	*xiii,* 68

Abstract

The Wnt/β-catenin pathway is a fundamental regulator of embryonic development and adult tissue homeostasis. The key effector, β-catenin, is a multifunctional protein that occupies dual roles in signalling and intercellular adherens junctions. β-catenin primarily signals though the TCF/LEF transcription factors; however, many transcription factors, in addition to TCF/LEFs, interact with β-catenin, and the function of these interactions is poorly understood. To investigate novel β-catenin regulated signalling mechanisms with certainty, we developed TCF/LEF quadruple knockout (QKO) mESCs. *In vitro* differentiation of QKO cells reveals a neural differentiation bias, which is attenuated by overexpression of stabilized β-catenin. Our data indicate the presence of a TCF-independent β-catenin regulated neural differentiation blockade in mESCs. In addition to directly challenging the central dogma of canonical Wnt signalling, this finding has the potential to unveil new therapeutic targets for the treatment of many β-catenin-associated diseases, including forms of brain cancer that may arise from the oncogenic stimulation of neural stem cells. Furthermore, we describe an attempt to identify genome-wide TCF-independent β-catenin binding sites in QKO cells by ChIP-seq. Optimization trials provide proof of concept that the fold enrichment method of interpreting ChIP-qPCR results can be highly misleading when compared to the more comprehensive % input method of analysis. This conclusion has important implications for all fields of scientific research in which ChIP-seq methodology is employed.

Acknowledgments

Foremost, I would like to express my sincere gratitude to my supervisor, Dr. Bradley Doble, whose motivation, expertise, understanding, patience, and guidance added considerably to my graduate experience. Dr. Doble's door was always open for when I had a question or obstacle. I could not have imagined a better supervisor and mentor for my studies. My experience in the Doble lab has fueled my immense academic and personal growth, and it will undoubtedly help to guide me in my future endeavours.

I would also like to thank my supervisory committee members, Dr. Eva Szabo and Dr. Darren Bridgewater, for their constructive feedback, helpful advice, and support throughout this process. Your advice and expertise played a pivotal role in my development as a scientist.

Special thanks to my fellow lab members for their encouragement and experimental contributions. I especially wish to thank Steven Moreira and Victor Gordon for working alongside me for the past three years and for helping me to troubleshoot experiments. Thanks also to Smarth Narula for taking over my project with much enthusiasm and determination.

My thanks and appreciation to the members of the Stem Cell and Cancer Research Institute (SCC-RI) for their help with experimental procedures, motivation, and friendship. I will miss you all.

I must thank my family and friends for their unwavering support throughout all my years of study. I could not have made it this far without their motivation and confidence in my abilities.

Finally, this work would not have been possible without the financial support of the Ontario Graduate Scholarship (OGS).

Table of Contents

List of Abbreviations vii
Declaration of Academic Achievement ix
CHAPTER 1: INTRODUCTION 1
1. Embryonic Stem Cells 1
1.1 Mouse Embryonic Stem Cells 1
1.1.1 Derivation *1*
1.1.2 Methods of Characterization *2*
1.2 Signalling Cascades Regulating mESCs 3
1.2.1 LIF/Stat3 ..... *3*
1.2.2 BMP4/Smad *4*
1.3 Non-canonical Wnt Pathways 5
1.3.2 The Planar Cell Polarity Pathway *6*
1.3.3 The Wnt/Ca^{2+} Pathway *7*
1.4 Canonical Wnt/β-catenin Pathway 7
1.4.1 Wnt Off State *7*
1.4.2 Wnt On State *9*
1.4.4 β-catenin *11*
1.5 Role of β-catenin in Pluripotency and Differentiation 13
1.6 β-catenin Signalling in Neurectodermal Differentiation 15
1.6.1 β-catenin-induced Neurectodermal Differentiation Blockade *17*
1.7 TCF-independent β-catenin Regulated Mechanisms 18
1.7.1 Non-TCF β-catenin Interacting Factors *20*
1.8 Project Rationale 21
CHAPTER 2: MATERIALS AND METHODS 23
1. Cell Culture 23
2. Sequencing of TCF/LEF loci 24
3. Generation of Stable β-catenin Overexpressing mESC Lines 24
4. EB Assays 24
5. Antibodies 25

6. Protein Lysate Preparation 25
7. Western Blot Analysis 26
8. Quantitative RT-PCR 26
9. Chromatin Immunoprecipitation Assay 27
10. ChIP-sequencing Data Analysis 28
CHAPTER 3: RESULTS 28
1. Biallelic Sequencing of TCF/LEF Indels in QKO mESCs 28
3. Generation of Stable β-catenin Overexpression Cell Lines 32
4. Overexpression of β-catenin in QKO mESCs Rescues the Neurectodermal Differentiation Bias in Vitro by a TCF-independent Mechanism 34
5. Identification of TCF-independent β-catenin Binding Sites in QKO mESCs 36
6. Optimization of β-catenin ChIP 39
CHAPTER 4: DISCUSSION 45
1. Summary of Findings 45
1.1 TCF-independent β-catenin-Regulated Neural Differentiation Blockade 45
1.2 β-catenin ChIP-seq 47
1.3 Doxycycline-inducible QKO Cell Lines 50
2. Potential Pitfalls and Alternative Approaches 50
2.1 TCF-independent β-catenin Regulated Neural Differentiation Blockade 50
2.2 β-catenin ChIP-seq 51
2.3 Doxycycline-inducible QKO Cell Lines 52
3. Future Directions 52
3.1 TCF-independent β-catenin Regulated Neural Differentiation Blockade 52
3.2 β-catenin ChIP-seq 53
3.3 Doxycycline-inducible QKO Cell Lines 53
4. Concluding Remarks 55
References 56

List of Abbreviations

	Abbreviation	Full Term
A	APC	Adenomatous polyposis coli
	ARM	Armadillo
B	BCBD	Beta-catenin binding domain
	BCL9	B-cell lymphoma 9
	bHLH	Pro-neural basic helix-loop-helix
	BMP	Bone morphogenetic protein
	β-TrCP	Beta-transducin repeats-containing proteins
C	C	Carboxy
	ChIP	Chromatin immunoprecipitation
	CK1	Casein kinase 1
	Co-IP	Co-immunoprecipitation
	CRD	Context-dependent regulatory domain
D	DKO	Double knockout
	DSB	Double stranded break
	Dvl	Dishevelled
E	E	Embryonic day
	EB	Embryoid body
	ECC	Embryonal carcinoma cell
	ESC	Embryonic stem cell
F	FGF	Fibroblast growth factor
	FZD	Frizzled
G	GFAP	Glial fibrillary acidic protein
	GP130	Glycoprotein 130
	GSK3	Glycogen synthase kinase
H	HA	Homology arm
	HAT	Histone acetyltransferase
	H&E	Hematoxylin & eosin
	hESC	Human embryonic stem cell
	HMG	High mobility group
I	ICM	Inner cell mass
	IF	Immunofluorescence
J	JAK	Janus kinase
K	K	Lysine
	Kbp	Kilobase pair
L	LEF	Lymphoid enhancer factor
	LRP	Low-density lipoprotein receptor-related protein
M	MAPK	Mitogen-activated protein kinase
	mESC	Mouse embryonic stem cell
	MNase	Micrococcal nuclease
N	N	Amino
	NES	Nuclear export signal

	NHEJ	Non-homologous end joining
	NLS	Nuclear localization signal
	NPC	Nuclear pore complex
P	PCP	Planar cell polarity
	Pygo	Pygopus
Q	QKO	Quadruple-knockout
S	S	Serine
	shRNA	Short-hairpin siRNA
	STAT	Signal transducer and activator of transcription
	SWI/SNF	SWItch/sucrose non-fermentable
T	T	Threonine
	TALEN	Transcription activator-like effector nuclease
	TLE	Transducin-like enhancer of split
W	WRE	Wnt-responsive element
	WT	Wildtype

Declaration of Academic Achievement

This thesis was completed mainly by Solen Abdulla, with the following contributions from individuals in Dr. Bradley Doble's lab:

i. Enio Polena developed the TCF/LEF quadruple knockout (QKO) cells;
ii. Jiayi Cao performed the EB assays analyzed in Figure 5;
iii. Steven Moreira cultured the cells analyzed in Figure 10;
iv. Smarth Narula generated the doxycycline-inducible construct in Figure 15A.

CHAPTER 1
INTRODUCTION

1. Embryonic Stem Cells

In 1963, James Till and Ernest McCulloch became the first to define the key properties of stem cells: self-renewal and differentiation (Mcculloch & Till 1963). Since their pioneering work, stem cell research has advanced the treatment of diseases such as cancer, revolutionized the field of regenerative medicine, and become a vital facet of the biomedical industry. Among those widely studied are embryonic stem cells (ESCs). ESCs are pluripotent, as defined by their ability to differentiate into cells of all three germ layers: ectoderm, endoderm, and mesoderm. Minimally, the transcription factors Oct4, Sox2, and Nanog comprise the core regulatory circuitry underlying the pluripotency and self-renewal of ESCs (Boyer et al. 2005).

1.1 Mouse Embryonic Stem Cells

1.1.1 Derivation

In early embryogenesis, the diploid zygote undergoes a series of cell divisions to form a structure called a blastocyst. By embryonic day 3.5 (E3.5), the blastocyst consists of about 64 cells that compose two main regions: the trophoblast and the inner cell mass (ICM) (Johnson 1981). The trophoblast becomes the trophectoderm after gastrulation and forms extraembryonic tissues such as the placenta, while the ICM develops into the embryo. ESCs are derived from the ICM of pre-implantation embryos. Prior to the successful isolation and propagation of mouse ESCs (mESCs), embryonal carcinoma cells (ECCs) obtained from the 129 strain of mice were used extensively as an *in vitro* model system for the study of early embryonic development (Przyborski et al. 2004). ECCs were used to

develop appropriate culture conditions for mESCs, leading to their derivation in 1981 (Kaufman 1981; Martin 1981). Upon isolation, mESCs were grown on feeder layers of embryonic fibroblasts to prevent spontaneous differentiation.

1.1.2 Methods of Characterization

There are several distinguishing characteristics of pluripotent cells. These cells have a high nucleus to cytoplasm ratio, distinctive nuclear and chromatin architecture, and rapid cell growth marked by an abbreviated G1 phase of the cell cycle (Becker et al. 2006). Murine pluripotent cells can be identified by cell surface antigens such as stage-specific antigen 1 (SSEA-1), alkaline phosphatase activity, unique microRNA (miRNA) profiles, and the core pluripotency transcription factors Oct4, Sox2, and Nanog (Houbaviy et al. 2003; Boyer et al. 2005). Lastly, pluripotent cells are unique in possessing distinct bivalent domains that contain both repressive and activating histone modifications (Azuara et al. 2006).

In addition to the defining characteristics of pluripotency, there are numerous functional assessments of the undifferentiated state. The gold standard tests of pluripotency are chimera formation and tetraploid complementation. In chimera formation, cells are injected into a mouse blastocyst and assessed for their contribution to the developing embryo (Okita et al. 2007). Cells contributing to all tissues of the organism are deemed pluripotent. Similarly, tetraploid complementation involves introducing cells into a 4n blastocyst, causing the resulting organism to be derived entirely from the introduced cells (Nagy et al. 1993). Another *in vivo* test involves the subdermal, intratesticular,

intramuscular, or kidney-capsule injection of putative pluripotent cells into mice, where they form tumours called teratomas (Gordeeva & Nikonova 2013). Teratomas with tissues from all three germ layers are indicative of pluripotent cells. Proof of pluripotency can also be obtained from the *in vitro* differentiation of ESCs. Differentiation can be spontaneous, in the form of embryoid bodies (EBs), or guided by defined culture conditions into specific cell types.

1.2 Signalling Cascades Regulating mESCs

Historically, mESCs were derived and maintained in fetal bovine serum (FBS)-containing medium on the substratum of mouse embryonic fibroblast (MEF) feeder cells. Two additional culture conditions have become increasingly prominent in recent years: 1) leukemia inhibitory factor (LIF)-supplemented FBS medium and; 2) serum-free culture containing two small molecule inhibitors (2i) targeting mitogen-activated protein kinase (MEK, PD0325901) and glycogen synthase kinase (GSK3, CHIR99021), respectively. mESCs can be maintained by stimulation from 3 main pathways: LIF, bone morphogenetic protein (BMP4)/Smad, and Wnt/β-catenin.

1.2.1 LIF/Stat3

A member of the interleukin-6 cytokine family, LIF binds to a heterodimeric receptor consisting of the low-affinity LIF receptor (LIFR) and Glycoprotein 130 (Gp130) (Ohtsuka et al. 2015). Gp130 activates a number of signalling pathways, including the Janus kinase/signal transducers and activators of transcription (JAK/STAT) pathway. In

this pathway, LIF-receptor binding leads to the autophosphorylation and activation of JAK, which in turn phosphorylates the transcription factor STAT3 (Shi & Massague 2003). Phospho-STAT3 dimerizes and translocates to the nucleus, where it activates pluripotency factors such as Oct4, Sox2, and Nanog. While LIF is required to sustain pluripotency in certain contexts, its effects are limited to certain genetic backgrounds, such as 129 inbred mice (Batlle-Morera et al. 2008). This strain-dependency can be overcome by LIF-independent 2i culture (Ying et al. 2008). Addition of LIF to 2i culture enhances pluripotency, indicating synergism between the three culture components (Ying et al. 2008).

1.2.2 BMP4/Smad

In contrast to LIF, which primarily inhibits mesendodermal differentiation, BMPs are well-known inhibitors of the neural fate (Ying et al. 2008; Wilson, P. A., & Hemmati-Brivanlou 1995). In feeder-free culture, BMP cooperates with LIF to maintain mESC pluripotency (Ying et al. 2003). Canonical BMP signalling is initiated by ligand-induced heterotetramerization of type I and type II serine/threonine kinase receptors (Wang et al. 2014). Upon activation, the type I receptor phosphorylates Smad1/5/8 (R-Smads), which associate with Smad4 to translocate to the nucleus and regulate gene expression. Notably, BMP/Smad signalling activates inhibitor of differentiation (Id) proteins, which suppress neural differentiation by binding and inhibiting pro-neural basic helix-loop-helix (bHLH) factors (Ying et al. 2003). In the non-canonical pathway, BMP further inhibits

differentiation by suppressing the extracellular signal-regulated kinase (ERK) 1/2 and P38 mitogen-activated protein kinase (MAPK) pathways (Qi et al. 2004).

1.2.3 Canonical Wnt/β-catenin

In 2i culture, CHIR99021 promotes cell proliferation and enhances pluripotency. CHIR99021 stimulates the Wnt/β-catenin pathway by inhibiting glycogen synthase kinase 3 (GSK3), a downstream component of the pathway that destabilizes β-catenin. Among its many functions, β-catenin translocates to the nucleus to alleviate TCF7L1-mediated repression of pluripotency genes such as *Nanog*, *Klf2*, and *Esrrb* (Atlasi et al. 2013; Hikasa et al. 2011; Shy et al. 2013). Interestingly, *Essrb* overexpression was shown to substitute for CHIR99021 in 2i culture, while genetic ablation canceled the effects of GSK3 inhibition (Martello et al. 2012). These findings reveal *Esrrb* as a key target of the Gsk3/TCF7L1 axis regulating pluripotency. The Wnt/β-catenin pathway will be discussed in greater detail below.

1.3 Non-canonical Wnt Pathways

The Wnt signalling pathways are a group of signal transduction cascades with crucial roles in embryonic development and adult tissue homeostasis (Wang & Nathans 2007; De 2011; Clevers 2006). There are at least three Wnt pathways: the canonical Wnt/β-catenin pathway and the non-canonical β-catenin-independent pathways, which are divided into the planar cell polarity (PCP) pathway and the Wnt/Ca^{2+} pathway. All Wnt pathways are modulated by Wnt ligands and converge on the common signalling component

Dishevelled (Dvl) (Gao & Chen 2010). Nineteen Wnt genes are present in the human and mouse genomes, which together constitute a family of lipid-modified, cysteine-rich, and highly hydrophobic glycoproteins (Nusse & Varmus 1992; Naylor et al. 2000; Kawano & Kypta 2003). Wnts that cause *Xenopus* axis duplication are labeled as canonical Wnts, and are assumed to function through Wnt/β-catenin signalling. The remainder of Wnts are labeled as non-canonical. Despite this classification system, Wnts are not autonomous, and there is considerable cross-talk between the pathways (Grumolato et al. 2010; Baksh et al. 2007).

1.3.2 The Planar Cell Polarity Pathway

The planar cell polarity (PCP) pathway is required for the proper establishment and maintenance of cell polarity in morphogenetic processes such as gastrulation and neural tube closure (Devenport 2014; Ueno & Greene 2003). Tissue-wide PCP is established by global cues such as secreted Wnt ligands, which bind to the Frizzled (Fz) receptor and a co-receptor such as Ryk, ROR1/2, or PTK7 (Martinez et al. 2015). Wnt binding leads to internalization of the ligand-receptor complex, followed by signal transduction through Dvl and downstream activation of c-Jun N-terminal kinase (JNK), Rho and Rac GTPases, and Rho-Kinase (ROCK) (Habas et al. 2003). These signal transduction cascades induce polarity by controlling rearrangements in the cytoskeleton and influencing gene expression. In addition to activating intracellular cascades, global PCP cues guide the asymmetric division of the vertebrate PCP transmembrane proteins Fz and Van Gogh

(Wu, J., & Mlodzik 2008). Polarity information is transmitted through intercellular PCP complexes to produce tissue patterning.

1.3.3 The Wnt/Ca^{2+} Pathway

The Wnt/Ca^{2+} pathway regulates morphogenetic processes such as gastrulation through the intracellular control of Ca^{2+} (De 2011). One of its key roles is promoting convergent extension (CE), a movement in which cells simultaneously elongate and intercalate at the midline. The Wnt/Ca^{2+} pathway is initiated via the binding of a Wnt ligand to the Fz receptor, which leads to the hyperphosphorylation and activation of Dvl. Activated Dvl triggers the activation of phospholipase C (PLC), a membrane-associated enzyme that cleaves phosphatidylinositol 4,5-bisphosphate (PIP2) into inositol triphosphate (IP3) and diacylglycerol (DAG). Upon binding to its receptor on the endoplasmic reticulum, IP3 causes Ca^{2+} to be released. Intracellular Ca^{2+} regulates cell adhesion and migration through the downstream activation of transcription factors such as nuclear factor of activated T-cells (NFAT).

1.4 Canonical Wnt/β-catenin Pathway

1.4.1 Wnt Off State

Stimulation of the canonical Wnt pathway by extracellular Wnt ligand leads to signal transduction through β-catenin, a key multifunctional protein effector that occupies dual roles in intercellular adhesion and signalling (Valenta et al. 2012; Clevers & Nusse 2012). In the absence of a Wnt signal, β-catenin is primarily found in adherens junctions, where it is bound by the transmembrane protein E-cadherin and intracellular proteins p120-

catenin and α-catenin (Hartsock & Nelson 2008). The non-junctional pool of cytosolic β-catenin is targeted for degradation by a large multiprotein assembly termed the 'destruction complex' (Stamos & Weis 2013; Hsu et al. 1999). The destruction complex is formed minimally by glycogen synthase kinase-3 (GSK-3), casein kinase 1 (CK1), β-Transducin repeats-containing proteins (β-TrCP), adenomatous polyposis coli (APC), and the scaffolding proteins Axin and Dishevelled (Dvl) (Stamos & Weis 2013; Hsu et al. 1999). CK1 initially phosphorylates β-catenin at serine (S) 45, priming GSK3 to phosphorylate threonine (T) 41, S37, and S33 (Marin et al. 2003; Taurog, R. E., Jakubowski, H., & Matthews 2006; Liu et al. 2002). Once phosphorylated, S33 and S37 function as critical components of the β-TrCP-binding site, allowing for the β-TrCP-mediated ubiquitination and subsequent proteasomal degradation of β-catenin (Aberle et al. 1997; Orford et al. 1997). This lack of available β-catenin allows for the downstream mediators of the pathway, termed the T-Cell Factor/Lymphoid Enhancer Factors (TCF/LEFs), to function as transcriptional repressors through interactions with corepressors such as those of the Groucho/Transducin-like enhancer of split (TLE) family (Figure 1) (Daniels & Weis 2005).

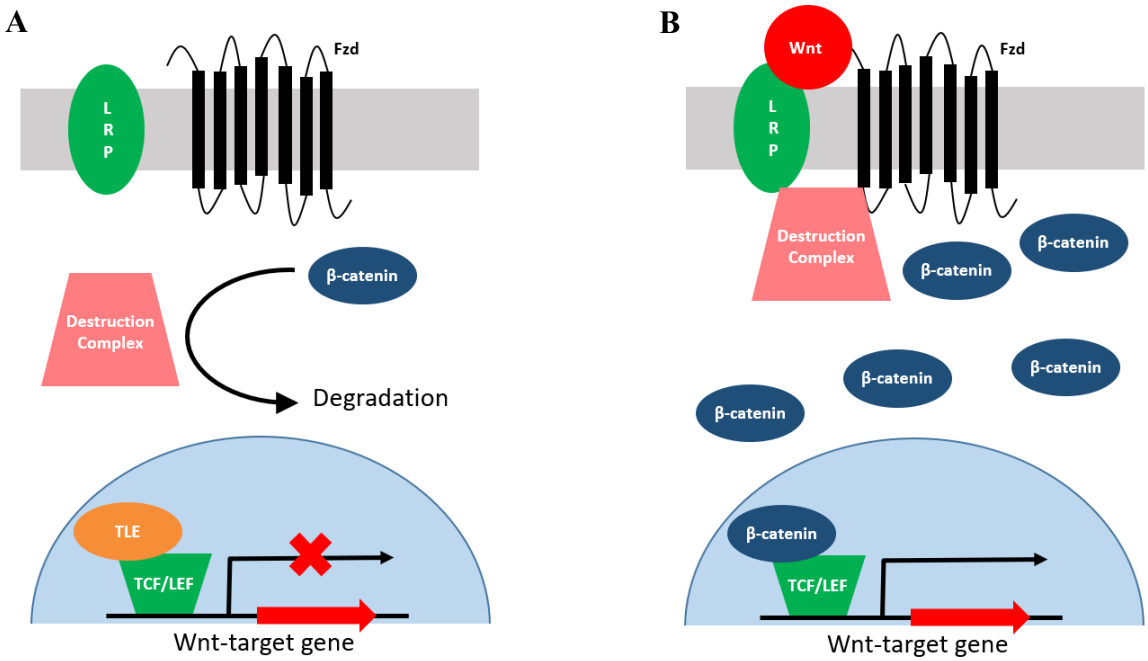

Figure 1. Canonical Wnt/β-catenin signalling. (A) In the absence of Wnt ligand, β-catenin is targeted for degradation by a cytosolic destruction complex. Nuclear TCF/LEF transcription factors, which are bound to corepressors such as those of the TLE family, repress the transcription of Wnt-target genes. (B) Upon binding of Wnt ligand to the Frizzled-LRP5/6 receptor complex, the destruction complex is recruited to the membrane and inactivated, thereby allowing for the cytosolic accumulation and nuclear translocation of β-catenin. Nuclear β-catenin binds to the TCF/LEFs to transactivate Wnt-target genes.

1.4.2 Wnt On State

The canonical Wnt/β-catenin pathway is initiated by the binding of Wnt ligand to a heterodimeric transmembrane receptor complex consisting of FZD and low density lipoprotein receptor-related protein (LRP) 5/6 (Naylor et al. 2000; Kawano & Kypta 2003b; Nusse & Varmust 1992). Activation of the co-receptor complex results in recruitment of the destruction complex to the membrane by Dvl and Axin, a process that is critical for deactivation of the complex (Tamai et al. 2004). Deactivation of the destruction complex ultimately allows for the cytoplasmic accumulation and nuclear

translocation of β-catenin (Angers & Moon 2009). After nuclear entry, β-catenin interacts with a variety of transcription factors, including members of the TCF/LEF family (Figure 1), to transactivate target genes (Angers & Moon 2009).

1.4.3 T-Cell Factors and Lymphoid Enhancer Factor

While most invertebrates carry a single TCF/LEF orthologue that occupies both transcriptional activation and repression roles, gene duplication and isoform complexity have led to specialized and novel structures, functions, and regulatory mechanisms in vertebrates (Klingel et al. 2012). In mice, the TCF/LEF family consists of TCF7 (TCF7), TCF7L1 (TCF7L1), TCF7L2 (TCF7L2), and LEF1 (Klingel et al. 2012). The general structure of TCF/LEF proteins is conserved within the animal kingdom such that all full-length TCF/LEF isoforms consist of a highly conserved amino-terminal β-catenin binding domain (BCBD), a variable context-dependent regulatory domain (CRD) containing a Groucho/TLE docking site, and an almost identical high mobility group (HMG) box by which TCF/LEFs bind the Wnt-responsive element (WRE, $^{A}/_{T}{}^{A}/_{T}$CAAAG) (Atcha et al. 2003; Atcha et al. 2007). In addition, the TCF7 and TCF7L2 contain a highly variable C-terminal 'E' tail, which imparts additional binding specificity to target genes (Figure 2) (Carlsson et al. 1993). Dual promoter usage and alternative splicing contribute to numerous TCF/LEF isoforms. In particular, alternative promoters lead to 'dominant negative' TCF7 and LEF1 isoforms, which lack the N-terminal β-catenin binding domain (Castrop et al. 1996; Weise et al. 2010). In general, the full-length isoforms of TCF7 and LEF1 are commonly associated with transcriptional activation (Reya et al. 2000; Yi et al.

2012). Contrastingly, TCF7L1 functions as a repressor of Wnt-target genes, while TCF7L2 can function as both an activator or repressor (Reya et al. 2000; Yi et al. 2012). Although the origin of these repressive functions is not well understood, the amino acid motifs LVPQ and SxxSS within the CRD of both TCF7L1 and TCF7L2 are believed to play a role.

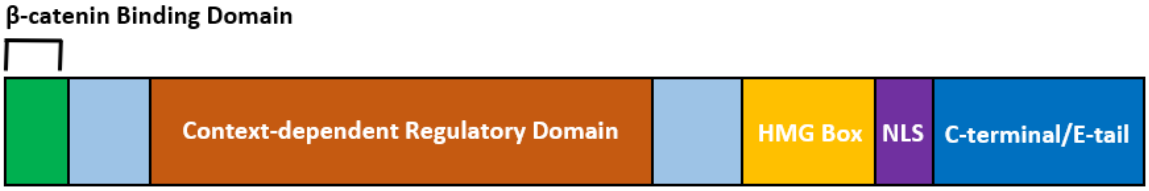

Figure 2. Schematic representation of TCF/LEF gene structure. Full-length TCF/LEFs can be divided into five distinct domains, including a β-catenin binding domain, HMG box, a nuclear localization signal, and a highly variable context-dependent regulatory domain. Additionally, some TCF/LEFs possess a C-terminal E-tail.

Upon Wnt activation, β-catenin interacts with TCF/LEFs in a poorly understood mechanism that results in the dissociation of repressive TCF/LEF-Groucho/TLE complexes from a subset of WREs, and subsequent transcriptional activation (Daniels & Weis 2005). This is referred to as the transcriptional 'switch'. TCF/LEFs are known for their ability to bend DNA between 90° and 127°, thereby facilitating interactions with distant transcriptional complexes (Giese et al. 1995).

1.4.4 β-catenin

In the late 1980s, the evolutionarily conserved β-catenin protein (781 amino acids in humans and mice) was independently discovered twice by its distinct structural and signalling roles (Nüsslein-Volhard, C., Wieschaus, E. and Kluding 1984). Soon after, in

the mid-1990s, several groups found that nuclear β-catenin/Armadillo signalling is primarily mediated by the TCF/LEF factors (Molenaar et al. 1996; Huber et al. 1997; Behrens et al. 1996). Because β-catenin lacks a DNA-binding domain, it must rely on DNA binding partners such as the TCF/LEFs to facilitate its transcriptional function. Adding to its unique structure, β-catenin lacks traditional nuclear localization (NLS) and nuclear export signals (NES) (Yokoya et al. 1999). Although the precise mechanism by which β-catenin enters and exits the nucleus is poorly understood, it is believed that β-catenin directly interacts with members of the nuclear pore complex (NPC) to mediate its translocation (Shitashige et al. 2008).

β-catenin is composed of three main functional domains that mediate its transcriptional output: the structurally rigid central Armadillo domain and the intrinsically disordered amino (N)- and carboxy (C)-terminal domains (Figure 3) (Huber et al. 1997). The central domain of β-catenin consists of 12 imperfect Armadillo (ARM) repeats that together form a super-helix with a long, positively charged groove. This positively charged groove constitutes the binding surface for over 20 β-catenin interacting partners, including the TCF/LEF factors, E-cadherin, and APC. Like the central domain, the N-terminal domain recruits various proteins that influence β-catenin's transactivation potential. For instance, the N-terminus contains a binding site for B-cell lymphoma 9 (BCL9), a scaffolding protein with transactivation properties that is capable of recruiting a coactivator termed Pygopus (Pygo) (Kramps et al. 2002). The N-terminus also contains an S33/S37/S45/T41 degron sequence, which upon phosphorylation, initiates the β-TrCP-mediated

ubiquitination and proteasomal degradation of β-catenin[36]. Downstream of the degron sequence exists a lysine-49 (K49) site, which represents a post-translational 'switch' for β-catenin function. Per the K49 switch, acetylated β-catenin K49 promotes the activation of target genes, while trimethylated β-catenin K49 results in gene repression. Although all three domains of β-catenin contribute to its transcriptional output, only the C-terminus is traditionally regarded as the 'transactivation domain'. The C-terminal domain recruits a multitude of proteins that influence transactivation potential, including histone acetyltransferases (HATs) and chromatin remodeling complexes of the SWI/SNF (SWItch/Sucrose Non-Fermentable) family (Kadam et al. 2003).

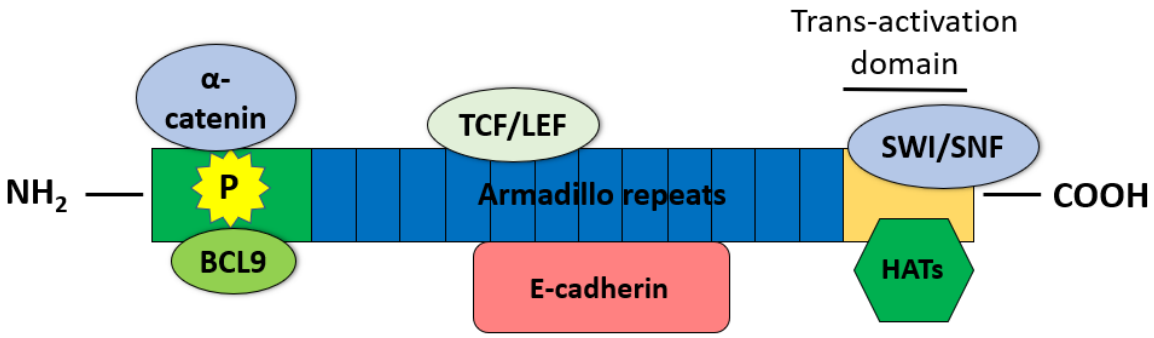

Figure 3. General schematic representation of β-catenin gene structure. WT β-catenin can be divided into three distinct domains: An N-terminal domain (green), which binds BCL9 and α-catenin and contains a phospho-degron sequence; a central Armadillo repeat domain (blue), which binds to the TCF/LEF factors and E-cadherin; and a C-terminal domain (yellow), which binds a multitude of transcriptional coactivators, including those of the HAT and SWI/SNF families.

1.5 Role of β-catenin in Pluripotency and Differentiation

The varied effects of Wnt/β-catenin signalling on ESC pluripotency have generated a great deal of controversy. In some cases, observed differences in pluripotency can be attributed to dissimilarities between mESCs and human ESCs (hESCs), which have

different gene expression signatures and require different culture conditions to maintain pluripotency (Ginis et al. 2004). In mESCs, Wnt/β-catenin signalling is known to both maintain pluripotency and to promote mesendodermal differentiation. These conflicting outcomes indicate a context- and time-dependent regulation by the signalling pathway.

The notion that Wnt/β-catenin signalling promotes pluripotency is supported by multiple models of β-catenin overexpression (Meijer et al. 2004; Doble et al. 2007; Kelly et al. 2011). For instance, genetic ablation of both GSK3α and GSK3β (double knockouts, DKOs) or CHIR99021-mediated inhibition of GSK3 enhanced pluripotency, as determined by the prolonged retention of ESC markers in teratoma and EB assays (Meijer et al. 2004; Doble et al. 2007). Surprisingly, however, GSK3 inhibition does not promote pluripotency through the upregulation of TCF/β-catenin target genes. To evaluate the role of TCF/β-catenin signalling in reinforcing pluripotency, Kelly and colleagues generated stable dominant-negative TCF7L2 (DN-TCF7L2)-expressing GSK3 DKO mESC lines (Kelly et al. 2011). Although the high-level TCF/β-catenin signalling observed in GSK3 DKO mESCs was heavily attenuated, pluripotency was still maintained. Similarly, overexpression of β-catenin$^{\Delta C}$, a β-catenin mutant lacking its C-terminal TCF-transactivating domain, sustained pluripotency and blocked differentiation in WT mESCs. One possible explanation for β-catenin's TCF-independent role in pluripotency involves OCT4, a core component of the transcriptional network regulating pluripotency. Specifically, β-catenin forms a complex with Oct4 and is associated with an increase in the transcription of Oct4 target genes (Kelly et al. 2011; Takao et al. 2007). Despite its

influence on pluripotency, β-catenin is dispensable for mESC maintenance. mESCs lacking β-catenin have normal self-renewal but display trilineage differentiation defects, demonstrating a requirement only for proper lineage commitment (Wray et al. 2011; Lyashenko et al. 2011).

Wnt/β-catenin signalling blocks neural differentiation and promotes mesendodermal differentiation in mESCs (Wray et al. 2011; Lyashenko et al. 2011). These Wnt/β-catenin-mediated cell fate decisions are highly context-specific and depend on the dynamic expression of Wnt receptors, ligands, antagonists, and other signalling components at different times during differentiation. However, the mechanism by which β-catenin counter-regulates mesendodermal and neural differentiation is poorly understood. Recently, Hoffmeyer and colleagues identified a β-catenin K49 "switch" that directs ESC differentiation. K49 of β-catenin can be trimethylated (β-catMe3) by enhancer of Zeste homolog 2 (EZH2) or acetylated (β-catAc) by CREB-binding protein (CBP), resulting in gene repression or activation, respectively (Hoffmeyer et al. 2017). β-catMe3 and β-catAc are differentially enriched at promoter regions of key mesendodermal and neural marker genes, thereby influencing ESC fate decisions.

1.6 β-catenin Signalling in Neurectodermal Differentiation

The central nervous system (CNS) is composed of three main neural cell types that are derived from neural stem cells: neurons, oligodendrocytes, and astrocytes. A neuron is a specialized cell that utilizes action potentials and neurotransmitters to transmit information to other neurons and all organs. In addition to playing important roles of their

own, oligodendrocytes and astrocytes, collectively termed glial cells, provide critical support for neuronal function and survival. Dynamic changes in the Wnt/β-catenin, Nodal, bone morphogenetic protein (BMP), and fibroblast growth factor (FGF) signalling pathways are involved in the proliferation of neural precursors and later in the terminal differentiation of neurons (Wen et al. 2009). The temporal and spatial interplay between these pathways, however, is still largely unclear.

The "neural default model" of embryonic development proposes that in the absence of cell-cell signalling, serum, or feeder cells, ectodermal cells will adopt a neural fate (Muñoz-sanjuán & Brivanlou 2002). In agreement with this model, mESCs grown in serum-free medium and the absence of feeder layers differentiated primarily into neurons (82%) (Tropepe et al. 2001). When seeded at higher densities, however, neural colony formation was inhibited. In vertebrates, BMP signal inhibition is required for the induction of neural differentiation (Tropepe et al. 2001). Neural induction is also facilitated by Nodal, FGF signaling, and Wnt/β-catenin signalling inhibition (Wilson et al. 2015). It has been postulated that inhibition of Wnt/β-catenin signalling indirectly promotes neural induction by simultaneously inhibiting mesendodermal differentiation and downregulating BMP4 (Baker et al. 1999). Following neural induction, BMP and Wnt/β-catenin signalling are required for neural precursor proliferation and the establishment of neural and glial lineages (Slawny & Shea 2011; Bond et al. 2013). Neural fate specification is driven in part by the key bHLH transcription factors Neurogenin1 and NeuroD1, both of which are transcriptional targets of canonical Wnt

signalling (Kuwabara et al. 2009). Wnt/β-catenin signalling may also influence neural patterning via poorly understood crosstalk with alternative signalling pathways (Wilson et al. 2015).

1.6.1 β-catenin-induced Neurectodermal Differentiation Blockade

Correlation between high levels of dominant-active β-catenin and inefficient tri-lineage differentiation has been observed in multiple mESC models (Kelly et al. 2011; Kielman et al. 2002; Haegele et al. 2003). To evaluate the effect of overexpressed β-catenin on differentiation potential, many studies have employed *in vitro* embryoid body (EB) assays. EBs are aggregates of differentiated cells, which recapitulate many features of early embryogenesis (Desbaillets et al. 2000). While wildtype (WT) mESCs generate descendants from all three germ layers in EB assays, our lab has found that GSK3α/β double knockout (DKO) mESCs and stable β-catenin S33A-overexpressing mESCs, both of which possess extremely high levels of β-catenin, show a lack of all three (Kelly et al. 2011). Notably, after 14 days of differentiation, DKO EBs displayed a complete lack of neuronal differentiation, as determined by immunofluorescent staining for β-III-tubulin and qRT-PCR analyses of neuronal markers. Similarly, β-catenin S33A-overexpressing mESCs displayed impaired neuronal differentiation. When injected into immunocompromised or syngeneic mice, WT ES cells form tumours known as teratomas, which are comprised of cells from all three germ layers. Contrastingly, DKO teratomas displayed an undifferentiated carcinomatous appearance, with the only differentiated structures consisting of spicules of bone derived from mesoderm. Further substantiating

the neuronal differentiation block in DKO EBs, DKO teratomas showed a complete absence of neural tissue, as confirmed by careful observation of hematoxylin and eosin (H&E) stained tissue sections, followed by immunostaining for the neural progenitor marker, Nestin, and astrocyte marker, Glial fibrillary acidic protein (GFAP).

To determine if elevated TCF/β-catenin-mediated transcription is responsible for the neuronal differentiation blockade, dominant negative TCF7 (DNTCF7) and TCF7L2 (DNTCF7L2) were stably expressed in DKO mESCs (Kelly et al. 2011). Stable expression of TCF7L2DN in DKO mESCs reduced the expression of TCF target genes to levels that were equivalent to those observed in DKO-GSK-3β mESCs. While DKO-GSK-3β mESCs were rescued in their ability to form neuronal tissue in EB and teratoma assays, DKO-TCF7L2DN mESCs maintained the differentiation block. Furthermore, DKO-TCF7L2DN mESCs were unable to differentiate in a defined neural differentiation assay. However, short-hairpin siRNA (shRNA) knockdown of β-catenin in DKO-TCF7L2DN mESCs eliminated the neuronal differentiation blockade. Together, these findings suggest that β-catenin restricts neuronal differentiation through either TCF-independent β-catenin regulated signalling or its cell adhesion function.

1.7 TCF-independent β-catenin Regulated Mechanisms

Multiple studies have attempted to separate the TCF-dependent signalling and cell-adhesion roles of β-catenin through the use of a C-terminal truncation mutant of β-catenin (β-catenin$^{\Delta C}$) (Kelly et al. 2011; Lyashenko et al. 2011; Takao et al. 2007). β-catenin$^{\Delta C}$

lacks the primary domain necessary for transactivation of β-catenin/TCF target genes but maintains its cell adhesion capacity. To explore the requirement for each function in germ layer formation, Lyashenko and colleagues compared the differentiation capacity of β-catenin$^{-/-}$ mESCs to those of β-catenin$^{\Delta C}$- and WT β-catenin-rescued mESCs (Lyashenko et al. 2011). While WT and rescue WT mESCs generate descendants from all three germ layers in EB assays, β-catenin$^{-/-}$ mESCs show a complete lack of all three. Interestingly, despite a lack of neurectoderm differentiation, expression profiles of the early ectodermal markers Nestin, Fgf5, and Pax6 were observed in β-catenin$^{-/-}$ mESCs during differentiation. Rescue of β-catenin$^{-/-}$ mESCs with β-catenin$^{\Delta C}$ restored neuroectodermal formation as determined by β-III-tubulin immunofluorescent staining, and endoderm formation as determined by immunofluorescent staining for Gata4, Foxa2, and Cxcr4. Together, these findings suggest that the β-catenin cell-adhesion function, rather than its TCF-dependent signalling function, is responsible for its role in ectoderm and endoderm differentiation.

Although β-catenin$^{\Delta C}$ has been widely used to assess β-catenin's cell-adhesion function, recent reports indicate that it may possess the ability to bind and regulate select non-TCF transcription factors. β-catenin$^{\Delta C}$ (694 aa) lacks much of the WT C-terminus but retains an N-terminal transactivation domain (Atlasi et al. 2013). Thus, it is plausible that β-catenin$^{\Delta C}$ can still bind to non-TCF/LEF proteins and recruit transactivating (and repressive) factors. In fact, our lab and others have shown that β-catenin$^{\Delta C}$ can bind to

Oct4 and enhance its activity as assessed by a palindromic Oct factor recognition element (PORE) reporter (Kelly et al. 2011).

1.7.1 Non-TCF β-catenin Interacting Factors

β-catenin primarily signals through the T-Cell Factor/Lymphoid Enhancer Factor (TCF/LEF) transcription factors; however, a poorly understood feature of β-catenin signalling is that many transcription factors, in addition to TCF/LEFs, interact with β-catenin. These interactions may expand β-catenin-regulated gene expression programs and provide an additional layer of crosstalk with other signalling pathways including the transforming growth factor beta (TGF-β)/Smad signalling pathway, the stress-activated protein kinase/c-Jun NH(2)-terminal kinase (SAPK/JNK) signalling pathway, and several nuclear receptor-signalling pathways (Valenta et al. 2012). Many non-TCF β-catenin-interacting factors have been shown to utilize β-catenin as a coactivator or corepressor to enhance their own transcriptional activity. These factors can also enhance or inhibit TCF/β-catenin signalling (Table 1). Often, a reduction in TCF/β-catenin-mediated transcription is attributed to competition between TCFs and non-TCF β-catenin interacting factors. The androgen receptor (AR), for instance, inhibits TCF/β-catenin signalling via this mechanism (Chesire & Isaacs 2002). At the expense of TCF/β-catenin signalling, β-catenin may function as a coactivator to promote the transcription of AR target genes in colon cancer cell lines (Schweizer et al. 2008).

Table 1. Non-TCF β-catenin Interacting Transcription Factors

Transcription Factor (TF)	Effect on TCF/β-cat Signalling	TF	Effect on TCF/β-cat Signalling	TF	Effect on TCF/β-cat Signalling
AP-1	+	GR	-	RAR	-
AR	-	HIF1α	-	RXR	-
E2F1	-	c-jun	-	Sox6	-
ERα	+	KLF4	-	Sox9	-
Foxo4	-	Lrh-1	-	Sox17	-
Foxo3a	-	Mitf	-	TRβ	-
FoxM1	+	Oct4	-	VDR	-
Gli3	-	PPARγ	-	Xsox3	-

1.8 Project Rationale

The long-term goal of this research project is to identify novel β-catenin regulated signalling mechanisms in mESCs. TCF-independent β-catenin signalling is poorly understood, and its study is limited by inadequate model systems. To study this form of signalling with certainty, we developed TCF/LEF quadruple-knockout (QKO) mESCs, which lack all four full-length isoforms of the TCF/LEF factors. We assessed the *in vitro* trilineage differentiation potential of QKO mESCs and identified a neural differentiation bias. Given that β-catenin overexpression impairs the neural differentiation of mESCs, we were interested in determining if this would attenuate the QKO neural differentiation bias. This thesis seeks to answer this question through the development and characterization of stable β-catenin S33A overexpressing QKO cell lines. This thesis also aims to identify

genome-wide TCF-independent β-catenin binding sites by performing chromatin immunoprecipitation followed by sequencing (ChIP-seq) on WT and QKO mESCs. Finally, this thesis documents the development of a doxycycline-regulated QKO cell line with inducible, stable expression of β-catenin S33A. This cell line has the potential to significantly advance our understanding of the non-canonical Wnt pathways by preventing cross-talk with the canonical pathway.

The experiments and future work outlined in this thesis will provide mechanistic insights into poorly understood β-catenin signalling mechanisms. A better understanding of β-catenin signalling may help to unveil new therapeutic targets for the treatment of β-catenin-associated diseases, including forms of brain cancer that may arise from the oncogenic stimulation of neural stem cells (Lee & Lee 2014; Singh, S.K. et al. 2004).

Hypotheses

1. Overexpression of stabilized β-catenin in QKO mESCs will inhibit neural differentiation.
2. TCF-independent β-catenin-mediated transcriptional regulation is a fundamental component of Wnt/β-catenin signalling.

CHAPTER 2
MATERIALS AND METHODS

1. Cell Culture

E14TG2a (ATTC® CRL-182™) mESCs were used to generate all derivative cell lines. Cells were stored in a humidified incubator (37°C, 5% CO_2), and cultured either on tissue culture plates coated with 0.1% gelatin or on plates containing a monolayer of feeder mouse embryonic fibroblasts. Standard maintenance media consisted of: Dulbecco's Modified Eagle Medium (DMEM, Sigma D5671) supplemented with 15% FBS (Gibco), 1X GlutaMAX (Gibco), 1 µM sodium pyruvate (Gibco), 1% non-essential amino acids (Gibco), 55 µM β-mercaptoethanol (Sigma), and 1000 U/mL mLIF (Miltenyi Biotec). Differentiation media used for embryoid body assays consisted of standard mESC media lacking mLIF. Cells were routinely propagated by washing once with phosphate buffered saline (PBS, Sigma), dissociating with Accutase (37°C, 5% CO_2, 5 minutes, Stem Cell Technologies), sedimenting by centrifugation at 1,500 x g for 2 minutes, and re-plating approximately once every two days, with a split ratio of 1 in 6. For experiments using N2B27 + mLIF 2i, mESCs were plated onto feeders for a single passage in standard mESC media and cultured for two passages on 0.1% gelatin-coated plates. Thereafter, mESCs were passaged on 0.2% gelatin-coated plates in N2B27 + mLIF 2i media: N2B27, 3 µM CHIR99021, 1 µM PD0325901, and 1000U/mL mLIF (Miltenyi Biotec). mESCs were maintained for three passages before being utilized for experiments.

2. Sequencing of TCF/LEF loci

Primers flanking CRISPR target sites were used to PCR amplify regions of interest. PCR products were separated on 1% agarose gels and extracted using the MiniElute Gel Extraction kit (Qiagen). Purified DNA was ligated into pJet1.2 (Thermo Scientific) and chemically competent bacteria were transformed with the constructs. DNA from 6 colonies was purified using the PureLink DNA Mini kit (Life Technologies) and sequenced by Sanger sequencing (Mobix, McMaster).

3. Generation of Stable β-catenin Overexpressing mESC Lines

Two million QKO mESCs and E14T mESCs were each transfected with 2ug of SalI-linearized pCAGGS-IRES-Puro-β-cateninS33A plasmid, which was obtained from Drs. Hiroshi Koide and Junichi Miyazaki. After 24 hours, cells were cultured for 24 hours in media containing 2 µM puromycin to select for cells containing the construct. Cells were then plated at clonal density in 10 cm plates and maintained in the absence of puromycin for 4-5 days, after which colonies were isolated, expanded, then collected for Western blot analysis.

4. EB Assays

Prior to the assay, cells were maintained on a monolayer of feeders in standard mESC medium for at least one passage. Hanging drop EBs were produced by depositing drops of 800 mESCs/30 µl EB medium onto the lids of 10 cm^2 petri dishes containing 10 ml of

sterile H_2O. After 3 days, EBs were transferred to ultra-low attachment 96-well plates (Corning). EB medium was replenished every 2 days.

5. Antibodies

The following primary antibodies were used for Western blot and/or immunofluorescent staining: mouse anti-β- Tubulin-I (T7816, Sigma); mouse anti-β-III-Tubulin (MAB1195, R&D Systems); mouse anti-mGAPDH (ab8245, Abcam); mouse anti-Myc Tag (05-724, Millipore); rabbit anti-GATA4 (sc-9053, Santa Cruz); HNF-3β (sc-374376, Santa Cruz); mouse anti-heavy chain cardiac Myosin (ab50967, Abcam).

6. Protein Lysate Preparation

After reaching 70-80% confluency, cells were washed once with 1x PBS, then incubated in radioimmunoprecipitation assay (RIPA) buffer [50 µM NaCl, 1% NP-40, 0.5% DOC, 0.1% SDS, 50 µM Tris pH. 8.0, 1 µM EDTA, and 1x Halt Protease Inhibitor Cocktail (Thermo Scientific)] for 10 minutes on ice. Lysed cells were then sedimented by centrifugation for 10 minutes at 16.1 x 10^3 x g at 4°C to isolate the supernatant. Protein concentration was determined using the DC Protein Assay (Bio-Rad) according to the manufacturer's protocol. Protein lysates were diluted to a final concentration of 0.5-1.0 mg/ml in 1x NuPage LDS Sample Buffer (Novex) and 5% Bond-Breaker TCEP (Novex), then heated at 95°C for 5 minutes prior to Western blot analysis.

7. Western Blot Analysis

Ten to 20 µg of protein per lane were separated through 8-10% Bis-Tris gels (150V, 1 hr). Proteins were transferred to polyvinylidene fluoride (PVDF) membranes using a Bio-Rad Mini TransBlot System (2hr, 200 mA) and Towbin transfer buffer (25 mM Tris, 192 mM glycine, and 20% (v/v) methanol). Membranes were blocked with 5% skim milk/tris-buffered saline (TBS) solution for 30 minutes to 1 hour at room temperature. Blocked membranes were incubated in primary antibody diluted in 3% skim milk/TBS-TWEEN® 20 (TBS-T) solution containing 0.5% TWEEN® 20 (Sigma) at 4°C overnight. After washing 3x15 minutes with 3% milk/TBS-T solution, membranes were incubated in horseradish peroxidase (HRP) conjugated secondary antibody for 45 minutes at room temperature. Membranes were then washed 3x20 minutes with TBS-T, and incubated in 25% Luminata Forte Western HRP Substrate (Millipore) for 5 minutes. Blots were visualized with the ChemiDoc MP Imaging System (Bio-Rad).

8. Quantitative RT-PCR

Total RNA was isolated using the PureLink RNA Mini Kit (Life Technologies), and 1 µg was transcribed into complementary DNA (cDNA) with qScript SuperMix (Quanta Biosciences). qRT-PCR reactions were produced using 3 µl cDNA (approximately 30 ng RNA) and SsoAdvanced SYBR Green SuperMix (BioRad). GAPDH was used as the reference gene. Relative gene expression was determined using the delta-delta Ct method in Bio-Rad's CFX96 software. Primer sequences were obtained from prior publications and are listed in Table 2.

Table 2. Qualitative qRT-PCR Primers

Primer	Sequence	Reference
Axin2	FWD: 5'-TTTGAGCCTTCAGCATCCTCCTGT-3'	(Doble et al. 2007)
	REV: 5'-AAGCCTGGCTCCAGAAGATCACAA-3'	
Brachyury	FWD: 5'-AGCTCTCCAACCTATGCGGACAAT-3'	(Kelly et al. 2011)
	REV: 5'-TGGTACCATTGCTCACAGACCAGA-3'	
mGAPDH	5'-CTTTGTCAAGCTCATTTCCTGG-3'	(Kelly et al. 2011)
	5'-TCTTGCTCAGTGTCCTTGC-3'	
SP5	5'-AACTACGACCCAGTTTCCTGTCCT-3'	(Kelly et al. 2011)
	5'-AGACATCTTTCCCAGCACCTTTGC-3'	

9. Chromatin Immunoprecipitation Assay

Chromatin immunoprecipitation (ChIP) assays were performed using the SimpleChIP Enzymatic Chromatin IP kit. Briefly, cells were cross-linked with varying levels of formaldehyde and/or ethylene glycol bis(succinimidyl succinate) (EGS), lysed, and treated with micrococcal nuclease (MNase) to fragment chromatin. Nuclei were lysed by sonication, and lysates in IP buffer were incubated overnight at 4°C with varying quantities of goat IgG and β-catenin antibody. Cross-linking was reversed by adding 6µl of 5 M NaCl to each IP and incubating overnight at 65°C. DNA was precipitated with ethanol and stored at −30°C for later use. Sequences of the ChIP primers for qRT-PCR are listed in Table 3.

Table 3. ChIP-qPCR Primers

Primer	Sequence	Reference
Axin2	FWD: 5' GTGCGCCAGCGGATCAATGGTGAGT 3'	(Zhang et al. 2013)
	REV: 5' AATAGCCGGCCTGCCAACTTCAAAG 3'	
Negative Control	FWD: 5' TGAATAAATGAAGGCGGTCCCA 3'	(Zhang et al. 2013)
	REV: 5' GGACCCTTGGTGCCCTACTA 3'	

10. ChIP-sequencing Data Analysis

Reads after sequencing were mapped against the mouse genome (NCBI build 37/ mm9) using Bowtie2 v.2.2.6 with the default parameters. Duplicate and unmapped reads were removed using Picard tools v.1.64 and reliable reads were indexed using Samtools v.0.1.18. BAM format outputs were sorted by genomic coordinates, then converted to BED files and finally to SlopBED files by Bedtools v.2.16.1. Bedtools was again used to convert SlopBED files to BEDgraph files, then to bigWig files. Using bigWig files as input, MACS14 called peaks and performed comparative analysis between controls and experimental samples.

CHAPTER 3
RESULTS

1. Biallelic Sequencing of TCF/LEF Indels in QKO mESCs

QKO mESCs were generated by employing CRISPR/Cas9 methodology to knock out all four full-length TCF/LEF factors in wild-type E14TG2a mESCs. CRISPRs were designed to target the first exon of each *TCF/LEF* gene (Figure 4A). Null alleles from all three QKO clones (i.e. QKO cl.A1, QKO cl.B8, and QKO cl.C2) were characterized by Sanger

sequencing (Figure 4B). Sequencing revealed small insertions or deletions (indels) that altered the reading frames and resulted in premature stop codons.

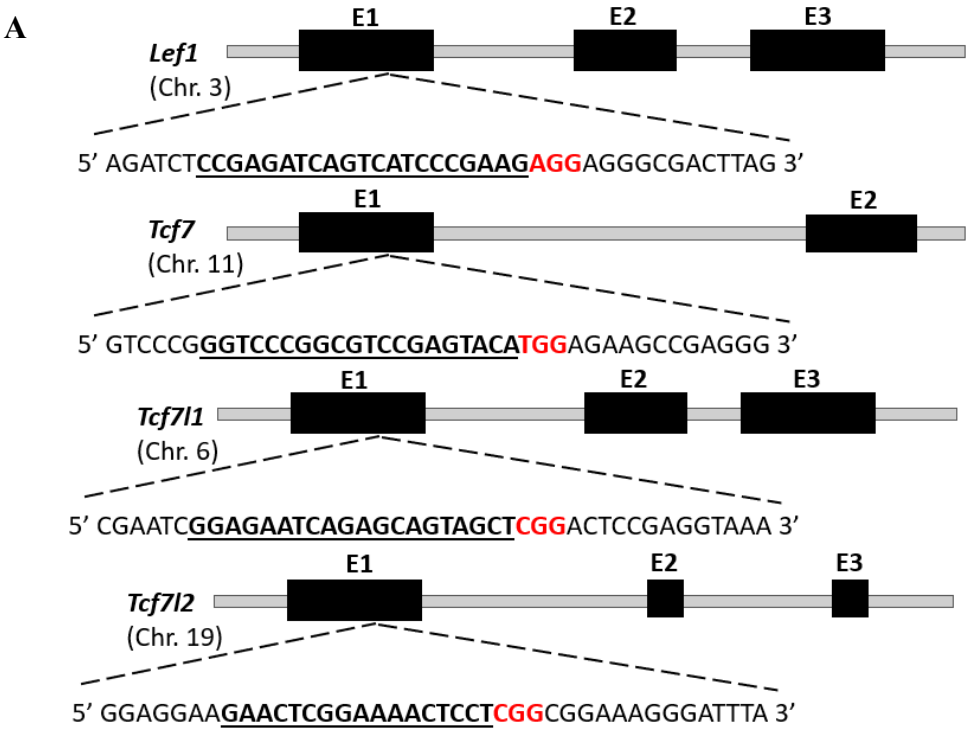

B

Lef1

5'	AGATCTTCGCCGAGATCAGTCATCCCGAAGAGGAGGGCGACTTAGCCGAC	3' **(WT)**
5'	AGATCTTCGCCGAG----------AGGAGGGCGACTTAGCCGAC	3' **(~16 bp)**
5'	AGATCTTCGCCGAGATCAG----------GAGGGCGACTTAGCCGAC	3' **(~13 bp)**

Tcf7

5'	GGCGCCGGGGTCCCGGGTCCCGGCGTCCGAGTACATGGAGAAGCCGAGG	3' **(WT)**
5'	GGCGCCGGGGTCCCG----------GAGAAGCCGAGG	3' **(~22 bp)**
5'	GGCCCCGGGGICCCG----------GAGAACCCGAGG	3' **(~22 bp)**

Tcf7l1

5'	AAGTCGTCCCTGGTCAACGAATCGGAGAATCAGAGCAGTAGCTCGGACTC	3' **(WT)**
5'	AAGTCGTCCCTG----------CTCGGACTC	3' **(~29 bp)**
5'	AAGTCGTCCCTGGTCAACG----------CTCGGACTC	3' **(~22 bp)**

Tcf7l2

5'	GAAGAACTCGGAAAACTCCTCGGCGGAAAGGGATTTAGCCGATGTCAAGT	3' **(WT)**
5'	GAAGAACTCGGAAAACTCCTtCGGCGGAAAGGGATTTAGCCGATGTCAAGT	3' **(+ 1 bp)**
5'	GAAGAACTCGGAAAACTCCTtCGGCGGAAAGGGATTTAGCCGATGTCAAGT	3' **(+ 1 bp)**

Figure 4. Biallelic sequencing of QKO mESCs. (A) Schematic of CRISPR design. CRISPR single guide RNA (sgRNA) sequences are underlined, and protospacer-adjacent motif (PAM) sites are shown in red. (B) Biallelic sequences of TCF/LEF indels in QKO mESCs. Adapted from: *Cell Reports* 20.10 (2017): 2424-2438.

2. QKO mESCs have Differentiation Deficits and Biases *in Vitro*

Four independent hanging drop EB assays were used to assess the trilineage differentiation potential of QKO mESCs. Western blot assays examined the markers β-III-tubulin (neurectoderm), Gata4 and HNF-3β (endoderm), and heavy chain cardiac myosin (mesoderm) at days 7 and 14 of differentiation (Figure 5). In comparison to WT EBs, QKO EBs displayed significantly lower levels of Gata4, HNF-3β, and heavy chain cardiac myosin at both time points. Contrastingly, QKO EBs displayed very high levels of β-III-tubulin. Taken together, the marker expression in QKO EBs is consistent with a neurectoderm bias and a mesendodermal differentiation blockade.

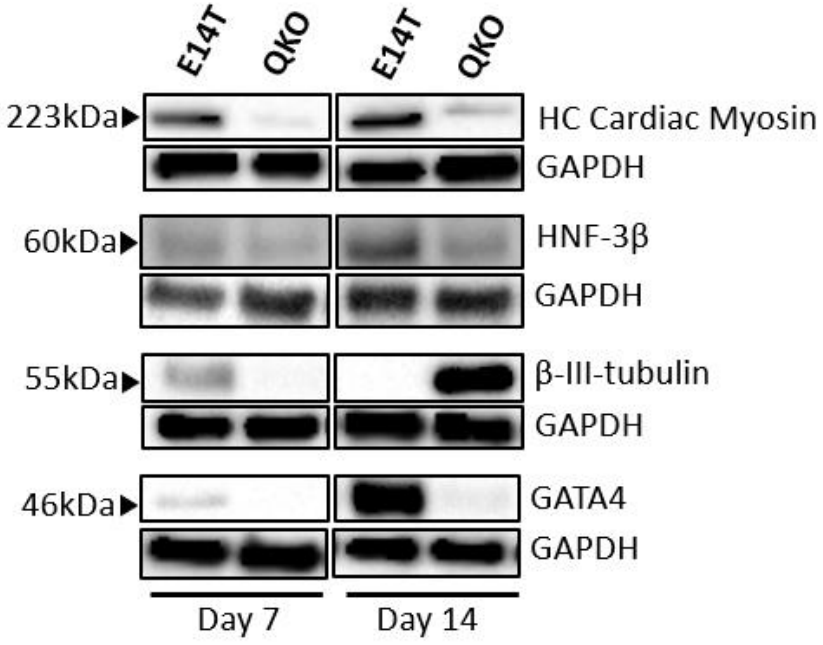

Figure 5. Protein expression levels of trilineage differentiation markers in day-7 and day-14 EBs. WT and QKO mESC lines were differentiated into EBs over 7 or 14 days and subsequently analyzed by Western blotting. GAPDH was used as a loading control.

3. Generation of Stable β-catenin Overexpression Cell Lines

Given that many β-catenin overexpressing cell lines display neurectodermal differentiation defects, we were interested in determining if β-catenin overexpression would attenuate the neurectoderm bias observed in QKO EBs. To address this question, we generated stable E14T and QKO cell lines overexpressing stabilized (S33A) β-catenin fused to a Myc tag. We obtained several independent cell lines in which Myc-β-catenin levels were equivalent to or greater than those detected in a previously characterized β-catenin-Myc overexpressing mESC line (E14K + Myc-β-catenin) (Figure 6A) (Kelly et al. 2011). Myc-β-catenin-expressing E14T and QKO mESCs were morphologically indistinguishable from their untransfected counterparts (Figure 6B).

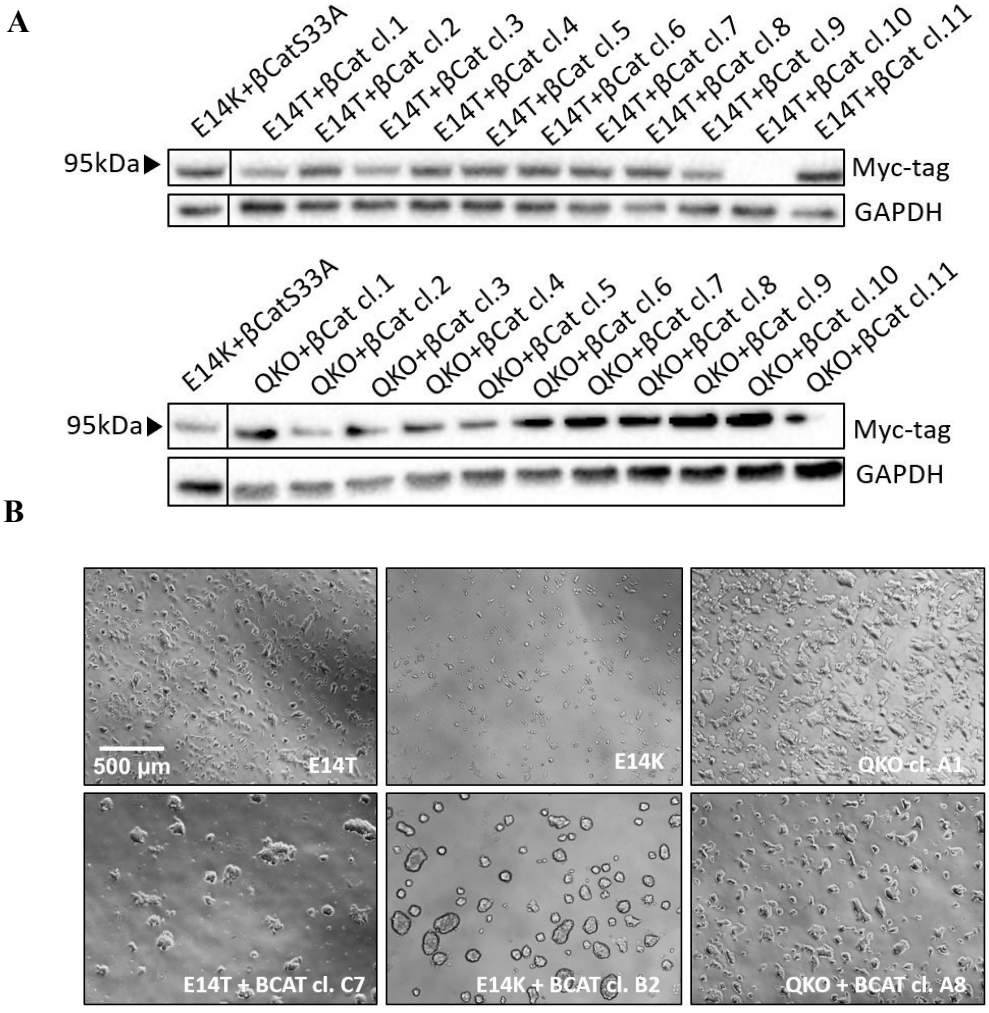

Figure 6. Generation of Myc-β-catenin S33A expressing mESC lines. (A) Protein expression levels of myc-β-catenin S33A. E14T and QKO mESCs were stably transfected with linearized Myc-β-catenin S33A expression vectors, and the resultant cell lines were analyzed by Western blotting. Myc-β-catenin S33A protein expression was observed at readily detectable levels from whole cell lysates of nearly all cell lines. GAPDH was used as a loading control. (B) Morphology of mESCs maintained in 15% FBS + LIF.

4. Overexpression of β-catenin in QKO mESCs Rescues the Neurectodermal Differentiation Bias *in Vitro* by a TCF-independent Mechanism

Four independent hanging drop EB assays were used to assess the trilineage differentiation potential of Myc-β-catenin-expressing EBs. By day 7-8 of differentiation, WT and WT + Myc-β-catenin cells developed into EBs with transparent cystic structures (Figure 7A). QKO and QKO + Myc-β-catenin cells never formed these transparent structures, developing instead into relatively small EBs with minimal projections.

Western blot assays examined protein levels of Myc-β-catenin and β-III-tubulin (neurectoderm) at days 7 and 14 of differentiation (Figure 7B). E14K, E14T, and QKO mESC lines expressing Myc-β-catenin expressed similar levels of Myc-β-catenin at day 7 of differentiation. By day 14, Myc-β-catenin was consistently upregulated in the E14T + Myc- β-catenin cell line but not the E14K+ Myc- β-catenin cell line. In contrast, Myc-β-catenin was consistently downregulated in both of the QKO + Myc-β-catenin cell lines. None of the cell lines expressed detectable levels of β-III-tubulin at 7 days. At 14 days, WT + Myc-β-catenin EBs still lacked the protein, while QKO EBs displayed very high levels. Interestingly, Myc-β-catenin overexpression significantly attenuated neural differentiation in day 14 QKO EBs. Taken together, marker expression in QKO + Myc-β-catenin EBs supports the presence of a β-catenin induced neural differentiation blockade that is governed by a TCF-independent mechanism.

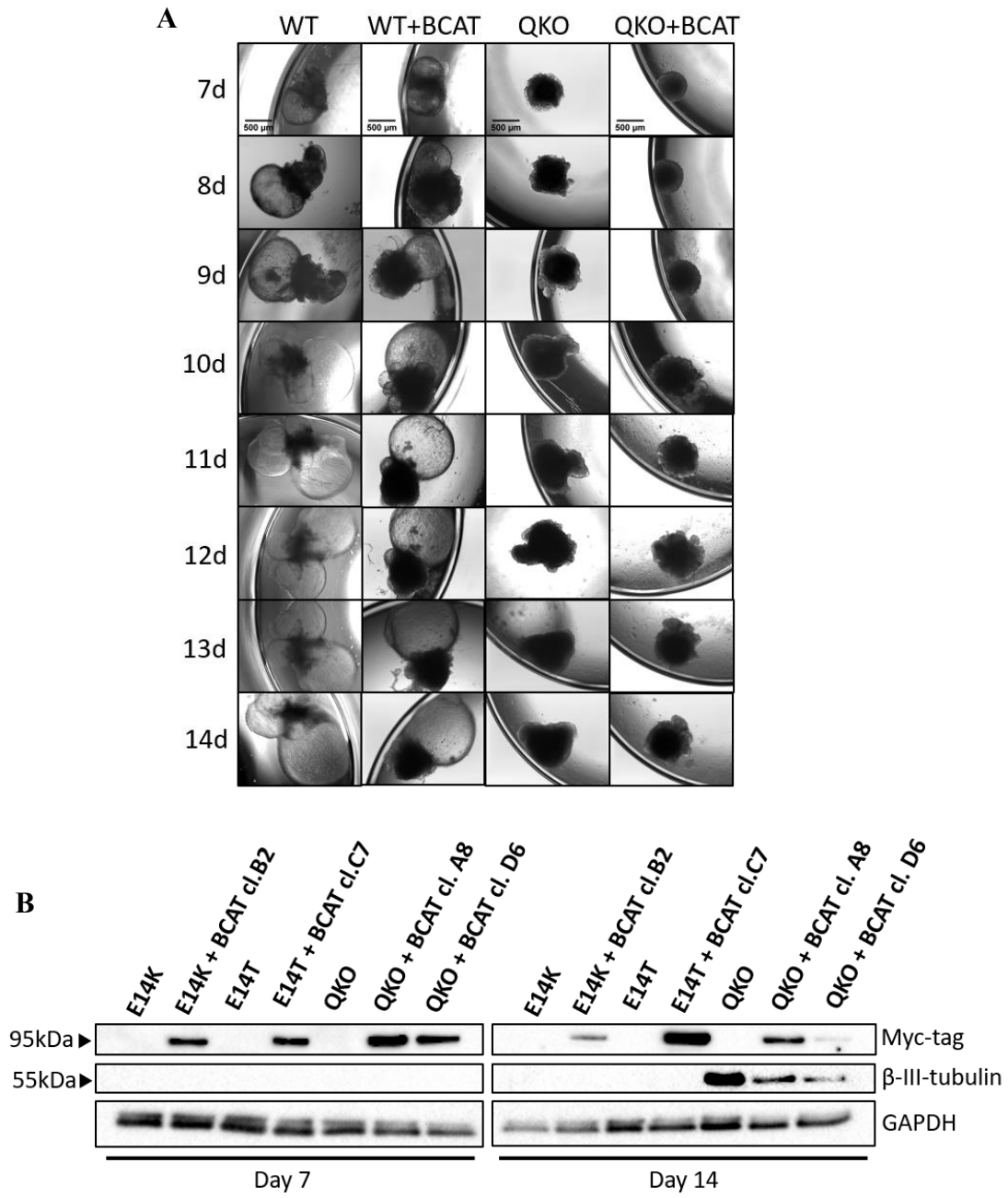

Figure 7. β-catenin overexpression attenuates neural differentiation in QKO EBs. (A) Morphology of EBs maintained in 15% FBS. (B) Embryoid bodies derived from the same number (800) of mESCs at various stages of differentiation. (B) Protein expression levels of β-III-tubulin in day-7 and day-14 EBs. mESCs were differentiated into EBs over 7 or 14 days and subsequently analyzed by Western blotting. GAPDH was used as a loading control.

5. Identification of TCF-independent β-catenin Binding Sites in QKO mESCs

Discovery of the TCF-independent β-catenin induced neural differentiation blockade gave us further reason to follow-up on the numerous reports of TCF-independent β-catenin signalling. To identify genes that are directly modulated by β-catenin in the absence of the TCFs, we employed chromatin immunoprecipitation followed by sequencing (ChIP-seq) as summarized in Figure 8. We performed ChIP-seq on two independent QKO mESC lines and one positive control WT mESC line, which were treated for 24 hours with the β-catenin-stabilizing drug, CHIR99021. After optimizing chromatin shearing to a uniform nucleosome ladder distribution (Figure 9A) and performing library preparation (Figure 9B), sheared ChIP DNA was sequenced and subjected to bioinformatic analysis (Figure 10). Analysis of the sequencing results revealed insignificant peak enrichment at many defined TCF/β-catenin binding sites in the WT mESC genome. These findings indicated a need for ChIP optimization.

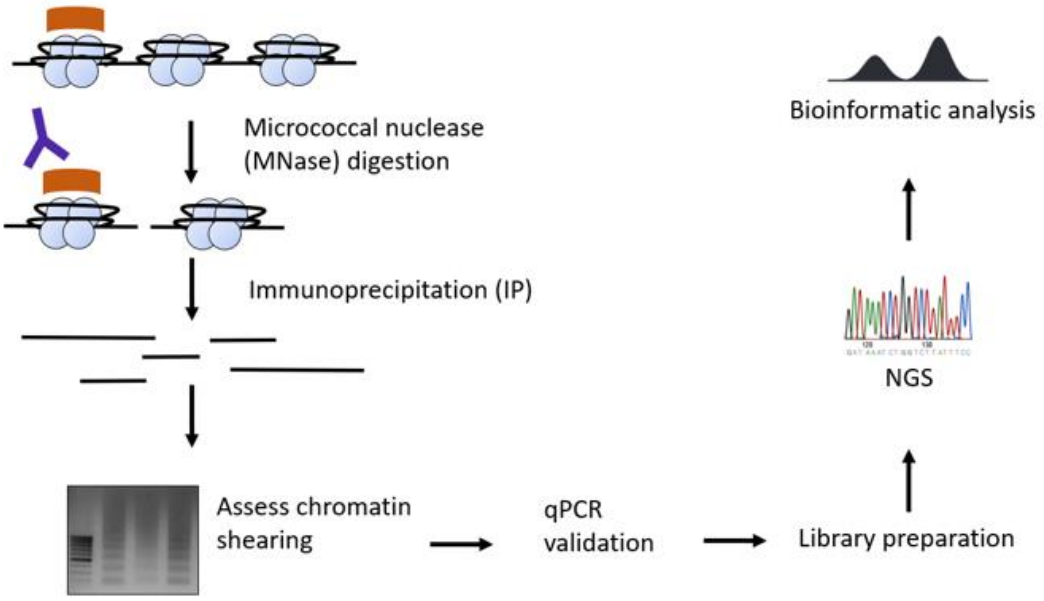

Figure 8: ChIP-seq workflow. Cells are fixed with formaldehyde and the chromatin is digested with MNase. Immunoprecipitations are performed using ChIP-validated antibodies. After the reversal of protein-DNA crosslinks, enrichment of target DNA sequences is assessed by qPCR. ChIP libraries are generated and sent for next generation sequencing (NGS) and bioinformatic analysis is performed using the raw sequencing data.

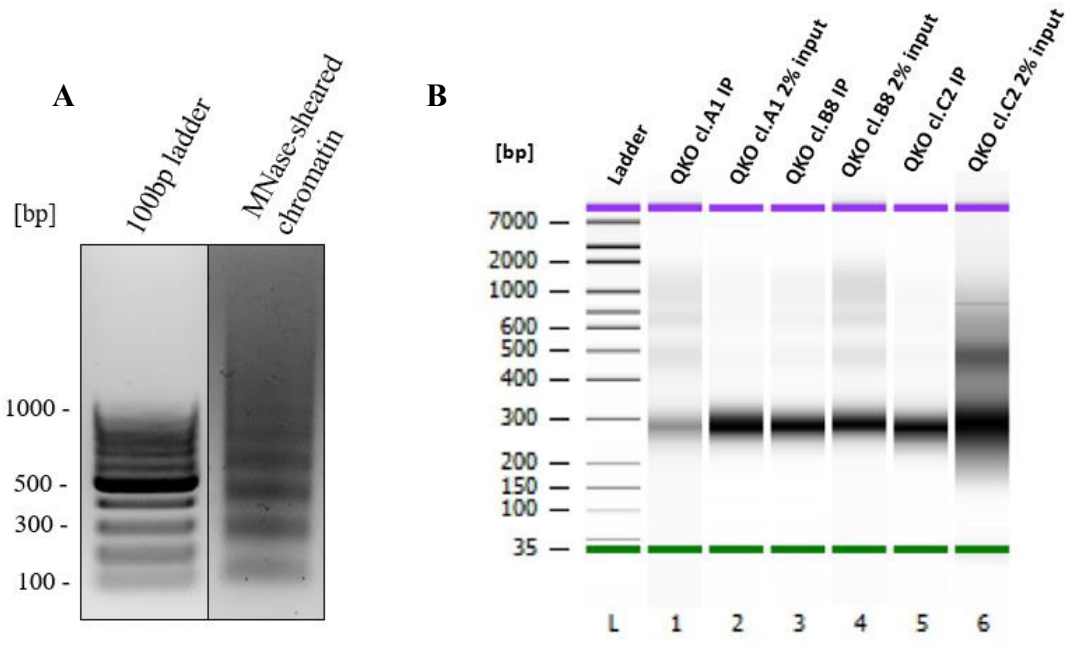

Figure 9. ChIP-seq library preparation. (A) MNase-based chromatin shearing. (B) β-catenin ChIP library preparation. Sheared, ChIP DNA and 2% input DNA from various cell lines were ligated to adaptor oligonucleotides and then PCR amplified to add unique barcode identifiers. Completed libraries were assessed by a bioanalyzer at the high sensitivity setting.

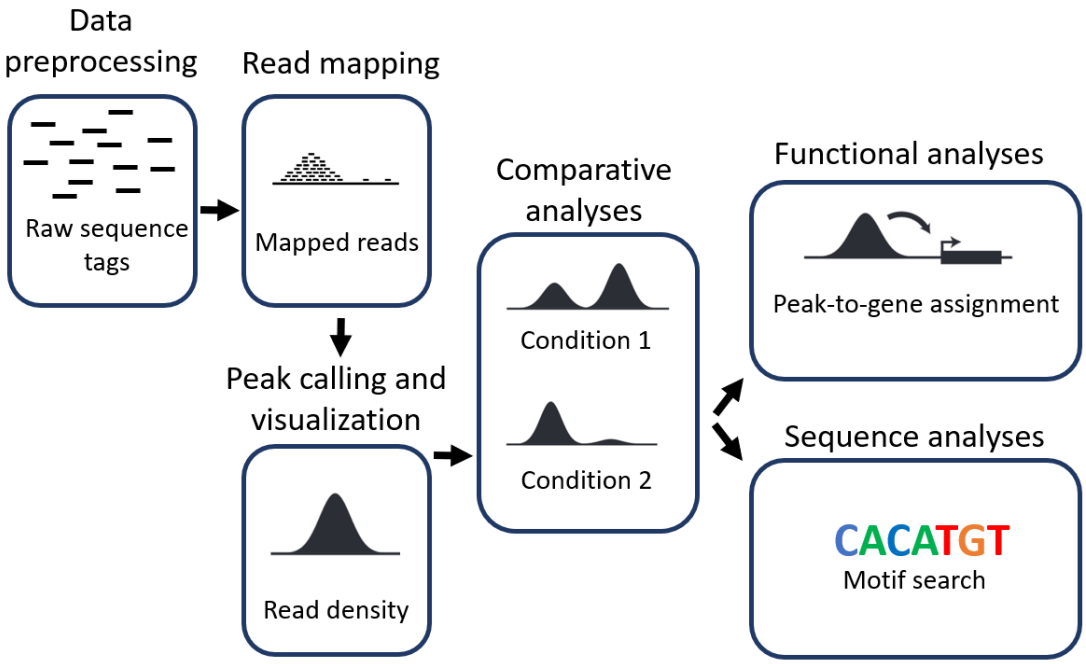

Figure 10: Computational pipeline for the analysis of ChIP-seq data. Raw reads are preprocessed and mapped to a reference genome. Peaks representing binding events are called by visualizing read densities. Comparative analyses can be performed between different cell lines, cell culture conditions, etc. Finally, functional analyses such as Gene Ontology (GO) and *de novo* binding motif analysis can be performed.

6. Optimization of β-catenin ChIP

To improve the ChIP protocol, we aimed to optimize three key aspects: (1) antibody and antibody concentration, (2) cross-linking conditions and; (3) level of chromatin shearing. The success of each ChIP trial was determined by the qPCR of sheared, uncrosslinked DNA. qPCR was used to evaluate the fold enrichment of select well-characterized TCF/β-catenin target loci, such as the TCF/β-catenin binding site in the promoter of *Axin2*. Furthermore, to ensure that E14T and QKO mESCs were responding appropriately to CHIR99021, we assessed the transcript levels of select Wnt/β-catenin target genes by qRT-PCR (Figure 11). As expected, QKO mESCs had a negligible response to both 3μM

and 10μM of CHIR99021. Contrastingly, WT mESCs showed a dose-dependent increase in the transcript levels of Wnt/β-catenin target genes.

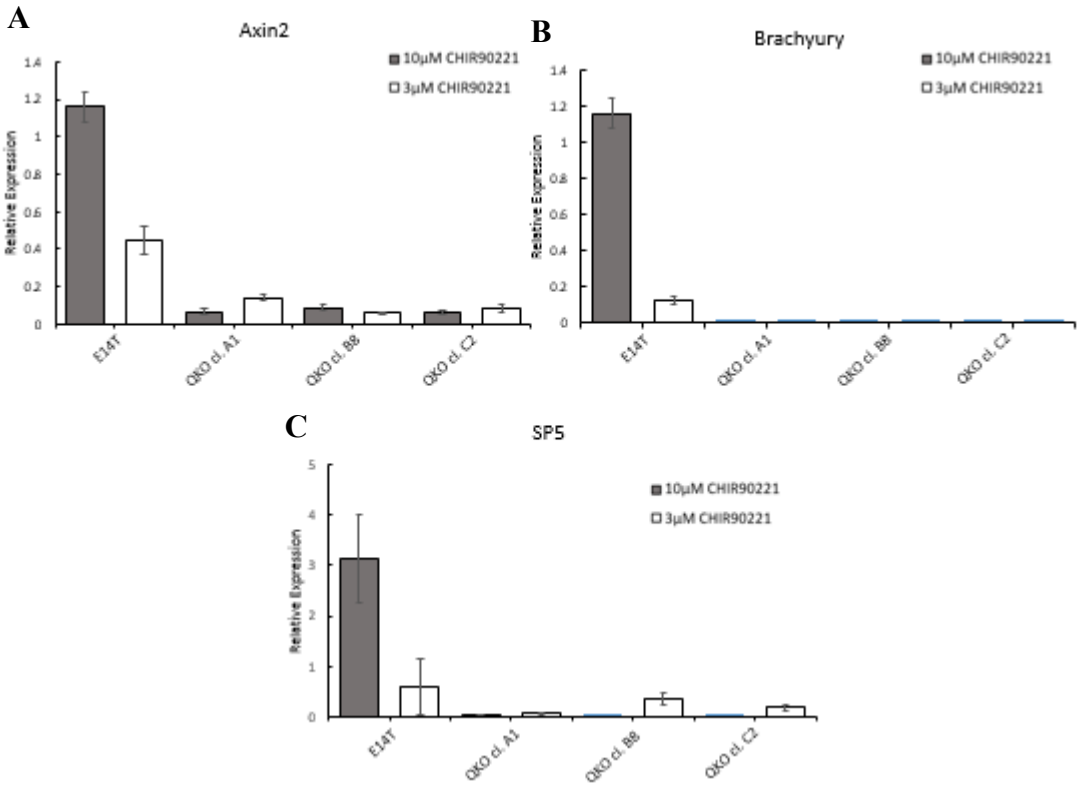

Figure 11. E14T mESCs respond appropriately to Wnt pathway activation. qRT-PCR analyses of mESCs maintained in 2i+LIF with 3μM or 10μM CHIR99021. Wnt pathway activation was measured by transcript levels of (A) Axin2, Brachyury, and SP5. Error bars = SEM.

The first optimization trial consisted of four different crosslinking conditions (Table 4). All four crosslinking conditions used formaldehyde, a commonly used crosslinking agent in ChIP. Two of these cases also used an additional crosslinking agent termed ethylene glycol bis(succinimidyl succinate) (EGS), which has been shown to aid in the ChIP of proteins, such as β-catenin, that do not directly bind DNA (Zeng et al. 2006). ChIP-qPCR results were assessed by two methods: (1) the fold enrichment method, which calculates enrichment relative to IgG control IPs and; (2) the % input method, which calculates

enrichment as a fraction of the total input DNA. According to the fold enrichment method, trial 4 (30 minutes of formaldehyde crosslinking) yielded the largest fold enrichment of about 50x, while trials 1-3 had relatively modest enrichments under 20x (Figure 12A). On the other hand, all trials had little to no enrichment at the negative control locus (Figure 12B). The % input method offered a drastically different interpretation of the results, as none of the 4 trials showed large enrichments at either the positive (Figure 12C) or the negative (Figure 12D) control locus relative to the IgG IP controls. As the % input method is a more comprehensive assessment of ChIP efficiency, all succeeding experiments were analyzed by this method.

Table 4. ChIP Crosslinking Trials

Trial	EGS	Formaldehyde
1	30 minutes	10 minutes
2	30 minutes	30 minutes
3	0 minutes	10 minutes
4	0 minutes	30 minutes

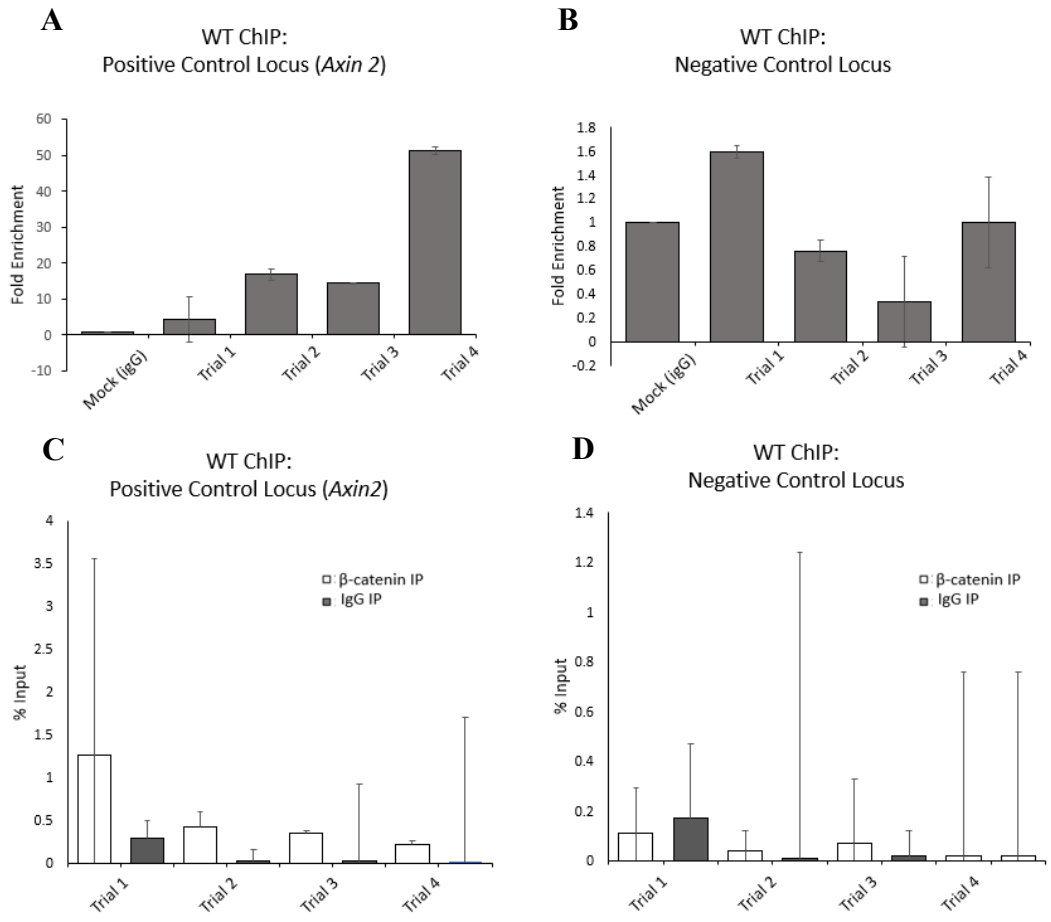

Figure 12. Comparison of fold enrichment method and % input method of ChIP-qPCR analysis. (A) Fold enrichment analysis of ChIP-qPCR at positive control locus (*Axin2).* (B) Fold enrichment analysis of ChIP-qPCR at negative control locus. (C) % input analysis of ChIP-qPCR at negative control locus. (D) % input analysis of ChIP-qPCR at negative control locus. Error bars = SEM.

To assess the impact of chromatin shearing on ChIP efficiency, we compared high vs. low shearing. Whereas high shearing involved an entirely mononucleosomal distribution at about 150bp, low shearing involved a uniform nucleosome ladder (Figure 13A). In the high shearing trial, both the β-catenin and IgG IP yielded no significant enrichment. In the low shearing trial, the positive control locus was detected at levels of approximately 4% input and 11% input in the β-catenin and IgG IPs, respectively (Figure 13B). Due to the

high background (IgG IP) observed in the low shearing trial, we decided to move forward with high shearing.

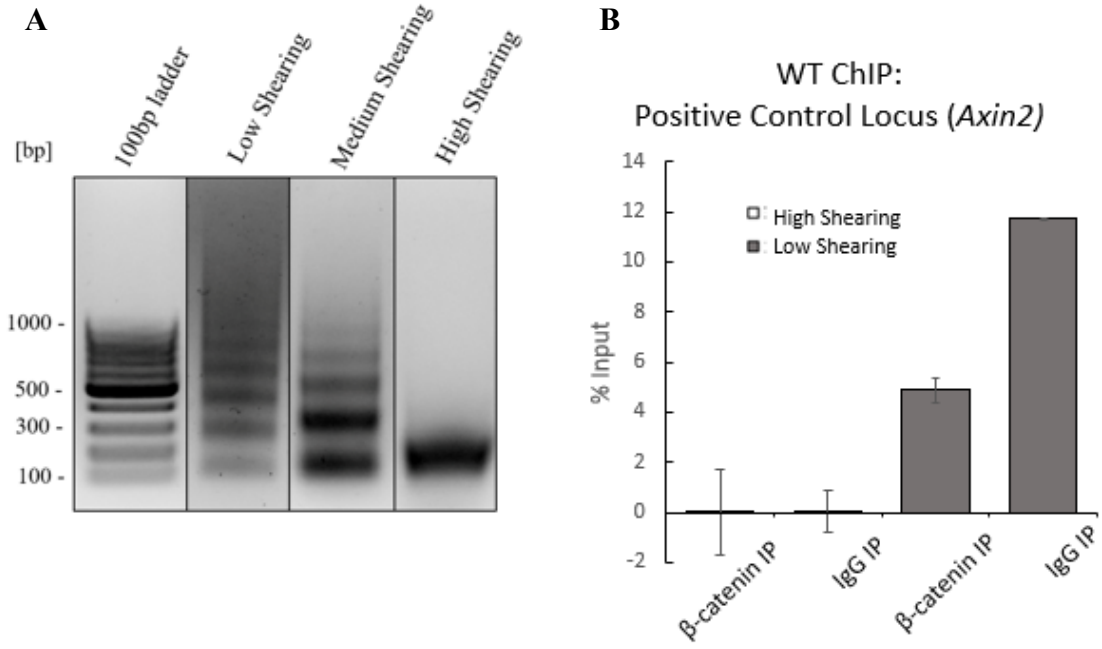

Figure 13. Optimization of MNase-based chromatin shearing. (A) Low, medium, and high-level chromatin shearing. (B) ChIP-qPCR analysis using the % input method. Error bars = SEM.

Finally, to optimize antibody concentration, we performed a ChIP trial with 4x the manufacturer's recommended quantity of antibody. The positive control locus was detected at levels of approximately 8% input and 2% input in the β-catenin and IgG IPs, respectively (Figure 14).

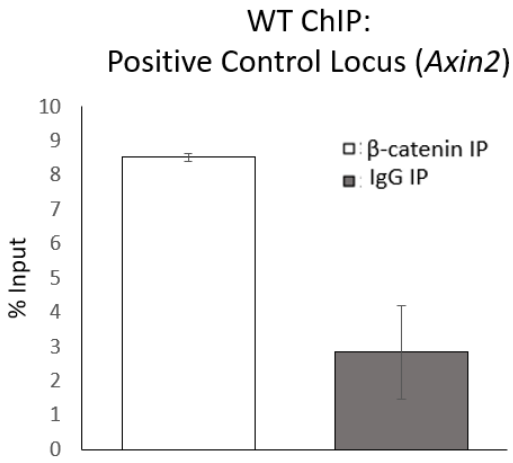

Figure 14. Optimization of antibody concentration. ChIP-qPCR analysis using the % input method. Error bars = SEM.

7. Development of a Doxycycline-regulated QKO Cell Line with Inducible, Stable Expression of β-catenin S33A

To date, the study of non-canonical Wnt signalling has been limited by inadequate model systems and by crosstalk with the canonical Wnt pathway. Our QKO cells represent a unique system in which to study non-canonical Wnt signaling mechanisms in isolation from β-catenin/TCF-mediated signalling. To eliminate crosstalk from β-catenin-mediated signaling, we aimed to knockout β-catenin in QKO cells. Furthermore, we wished to assess the role of β-catenin in modulating the transcriptional output of "non-canonical" Wnts. Thus, we designed a doxycycline-regulated construct with inducible, stable expression of β-catenin S33A (Figure 15A). This expression construct was delivered to the Rosa26 locus of QKO cells by transcription activator-like effector nucleases (TALEN)-mediated gene targeting. Resultant mESC colonies were isolated and screened

for the presence of the construct in groups of 3 (Figure 15B). The PCR-based screen showed a very high efficiency of genomic integration.

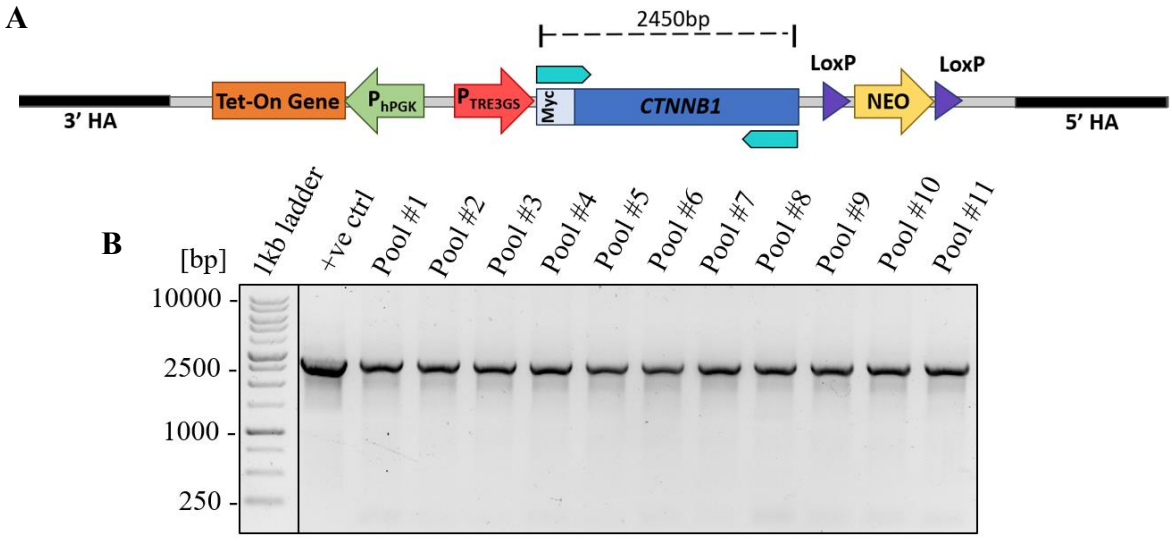

Figure 15. PCR-based screen for doxycycline-regulated Myc-β-catenin expression construct. (A) Schematic of doxycyclin-regulated Myc-β-catenin expression construct. PCR screen primers (light blue) and the expected band size are depicted. (B) PCR-based screen for Myc-β-catenin. Following transfection, 33 neomycin-resistant mESC clones were isolated. Groups of 3 colonies were pooled and screened for the presence of Myc-β-catenin.

CHAPTER 4
DISCUSSION

1. Summary of Findings

1.1 TCF-independent β-catenin-Regulated Neural Differentiation Blockade

We generated stable Myc-β-catenin expressing E14T and QKO cell lines to investigate the neural differentiation bias observed in QKO EBs. These cell lines were indistinguishable from E14T and QKO cells, respectively. Western blot analyses showed

that Myc-β-catenin overexpression significantly attenuated protein levels of β-III-tubulin in day 14 QKO EBs (Figure 7B). These findings suggest that neural differentiation is inhibited solely or in part by a TCF-independent β-catenin mechanism. This mechanism could represent β-catenin's cell adhesion role or β-catenin's TCF-independent signalling role.

Despite expressing similar levels of Myc-β-catenin (Figure 6A), E14T + Myc-β-catenin and QKO + Myc-β-catenin cell colonies differ drastically from E14K + Myc-β-catenin cell colonies, which display highly refractile, spherical, and tightly packed colonies of the Myc-β-catenin expressing E14K + Myc-β-catenin cell line (Figure 6B). The Myc-β-catenin expressing E14T and QKO cell lines behaved similarly to previously characterized β-catenin overexpressing lines, which also showed no change in morphology from their untransfected counterparts (Otero et al. 2004). Given that the E14K + Myc-β-catenin cell line was generated by random integration, it is possible that its morphology was impacted by disruption of a gene encoding a vital protein, such as a cytoskeletal component.

The neural differentiation bias observed in QKO EBs is consistent with the notion that lack of TCF/β-catenin signalling indirectly promotes the neural lineage by inhibiting mesendodermal fate determination (Aubert et al. 2002). This notion is supported in part by embryos lacking β-catenin, Wnt ligands, or LRP5/6 co-receptors, in which neurectoderm develops at the expense of mesendoderm (Huelsken et al. 2000; Kelly et al.

2004; Albrecht et al. 2014). Furthermore, given the numerous reports of β-catenin-mediated inhibition of neural induction (Kelly et al. 2011; Atlasi et al. 2013; Doble et al. 2007), we were not surprised to observe the TCF-independent β-catenin induced neural differentiation blockade in Myc-β-catenin expressing QKO EBs. Due to β-catenin's pleiotropic functions, it is difficult to ascertain the source of the neural differentiation blockade. One possible explanation for this phenomenon involves crosstalk between the β-catenin and Notch signalling pathways. Shimizu and colleagues showed that β-catenin can bind Notch1 and transactivate its target genes in mESCs (Shimizu et al. 2008). The most notable of these targets was the anti-neurogenic gene *Hes1*. Hes1 promotes the proliferation of neural precursor cells, while simultaneously inhibiting neural differentiation. Thus, β-catenin/Notch1 mediated upregulation of *Hes1* is a plausible explanation for the TCF-independent neural blockade observed in this thesis.

1.2 β-catenin ChIP-seq

In summary, we performed β-catenin ChIP-seq and obtained an inadequate peak enrichment at many defined TCF/β-catenin binding sites in the WT mESC genome. We improved the ChIP protocol by optimizing antibody and antibody concentration, crosslinking conditions, and the degree of chromatin shearing. Finally, we provide proof of concept that the fold enrichment method of interpreting ChIP-qPCR results can be highly misleading when compared to the more comprehensive % input method. Insignificant peak enrichment in the β-catenin ChIP-seq experiment indicated a need for optimization of ChIP. It is generally accepted that a successful ChIP-seq experiment

depends on a minimum 10-fold enrichment over an IgG control. To attain this level of enrichment, we optimized key components of the ChIP protocol: (1) antibody and antibody concentration, (2) crosslinking, and (3) chromatin fragmentation. First, we obtained an improved, ChIP-approved β-catenin antibody to conduct the optimization trials. The crosslinking trials consisted of varying crosslinking intensities, from very little crosslinking to very high crosslinking. We also incorporated an atypical crosslinking agent called EGS, which performs well with proteins such as β-catenin, which do not directly bind DNA. EGS is a relatively large molecule with a wide spacer arm, making it optimal for this purpose (Zeng et al. 2006). Since none of the crosslinking conditions resulted in a large enrichment, the problem was likely not to do with crosslinking. The next optimization trial aimed to determine the optimal level of chromatin fragmentation. Although low fragmentation yielded an enrichment of ~5% input in the β-catenin ChIP, the corresponding IgG ChIP displayed a much larger enrichment. This indicated that most, if not all, of the enrichment calculated in this experiment was due to non-specific binding to the protein G magnetic beads used in the protocol. Unlike low chromatin fragmentation, the high chromatin fragmentation trial resulted in no significant enrichment in either the β-catenin or IgG ChIP. The final optimization trial assessed the impact of antibody concentration on ChIP efficiency. Four times the manufacturer recommended quantity of antibody was used in this trial. This trial yielded the most promising results in the optimization process, with enrichments of ~8% and ~2% input in the β-catenin ChIP and IgG IP, respectively.

The ChIP optimization trials reveal many possible avenues for improving the protocol. One possible explanation for suboptimal results is a poor antibody. Since even a four-fold excess of antibody did not yield an acceptable enrichment, this is a plausible explanation. It is also possible that overheating of the samples caused the degradation of isotopes, which would have led to poor recognition by the antibody. Overheating may have stemmed from incubating samples at 37°C for MNase digestion, or by sonication-based nuclear lysis. To circumvent these potential issues, sonication-based chromatin fragmentation and an isothermal nuclear lysis technique could be applied, respectively. Finally, the relatively large enrichment in IgG control ChIPs indicated high levels of non-specific binding to the protein G beads. The β-catenin:IgG ChIP enrichment ratio could be improved by interventions such as blocking the protein G beads or conducting more stringent wash steps.

The method of data normalization can have a major impact on the interpretation of ChIP-qPCR results. Currently, the two most common methods of normalization are the fold enrichment method and the % input method (Haring et al. 2007). Whereas the fold enrichment calculation indicated a ~50x enrichment in trial 4 of Figure 12, the % input calculation indicated a very minimal enrichment of ~0.22% input. The fold enrichment method represents the ChIP signal as the fold increase relative to the background signal (IgG ChIP). This method assumes that the level of background signal is reproducible over replicate experiments and primer sets. As demonstrated in this thesis, background levels can differ dramatically between samples. For this reason, the fold enrichment method is

highly prone to incorrect data interpretation. In contrast to this method, the % input method represents the ChIP signal as a percentage of the total input DNA. The main disadvantage of this method is that it assumes both the input and ChIP samples were handled in the same way. Although they are generally handled similarly, the input sample is isolated early in the ChIP procedure and processed separately from the ChIP samples. Overall, the % input method is a more comprehensive normalization method because it allows for comparison between both the input and IgG ChIP samples, rather than only the IgG ChIP samples.

1.3 Doxycycline-inducible QKO Cell Lines

We have nearly generated doxycycline-regulated QKO cell lines with inducible, stable expression of β-catenin S33A. The preliminary PCR-based screen for the expression construct showed a very high rate of integration into the genome (Figure 15B). To ensure that these clones did not reflect random integration events, we will screen for proper homologous recombination by subsequent PCR screens targeting the 3' and 5' homology arms.

2. Potential Pitfalls and Alternative Approaches

2.1 TCF-independent β-catenin Regulated Neural Differentiation Blockade

It is possible that β-catenin does not regulate neural differentiation through transcriptional activation or cell adhesion, but rather through a post-transcriptional mechanism at the RNA or protein level. For instance, β-catenin has been shown to cooperate with Oct4 in

an epigenetic mechanism that leads to the promotion of mesendoderm differentiation (Ying et al. 2015). Thus, instead of solely focusing on the transcriptional activation function of β-catenin, it will be helpful to consider such alternative possibilities in future experiments.

2.2 β-catenin ChIP-seq

There is a chance that β-catenin does not bind and regulate genes in the absence of the TCFs. However, given the numerous non-TCF-β-catenin interacting transcription factors (Table 1), this is unlikely. Nevertheless, as GSK3 has at least 100 putative substrates (Sutherland 2011), the proposed experiments would shed light on the non-TCF-related effects of CHIR99021 on the mESC transcriptome. Furthermore, it is possible that β-catenin ChIP will be optimized for TCF/β-catenin DNA-binding in WT mESCs but not for non-TCF/β-catenin DNA-binding in QKO mESCs. This is because there are currently no well-characterized TCF-independent β-catenin binding sites at which to evaluate ChIP efficiency. However, if the bioinformatic analysis does not reveal any significant non-TCF/β-catenin DNA-binding sites, ChIP can again be optimized with the aim of capturing these loci. An additional pitfall of the study is that QKO cells retain the dominant negative isoforms of the TCF/LEF factors. All TCF factors except for TCF7L1 have N-terminally truncated variants that lack the β-catenin binding domain (Vacik et al. 2011). These isoforms retain the ability to enter the nucleus and displace β-catenin by occupying TCF/β-catenin binding sites. This may interfere with the identification of nuclear β-catenin binding proteins that also associate with the TCFs.

2.3 Doxycycline-inducible QKO Cell Lines

It is possible that the non-canonical Wnt pathways function primarily to inhibit Wnt/β-catenin signalling. In this case, the effects of the non-canonical Wnts would require intact TCF/β-catenin signalling. Although we believe that this is unlikely, this information alone would be very informative and would warrant follow-up studies.

3. Future Directions

3.1 TCF-independent β-catenin Regulated Neural Differentiation Blockade

Future work will aim to elucidate the precise mechanism by which β-catenin regulates target genes to promote the neural differentiation blockade. To identify global transcriptional changes that occur in stable β-catenin S33A overexpressing QKO mESC lines versus their untransfected counterparts (controls), we will perform RNA-seq. A subset of differentially expressed genes will be selected according to their relevance to neural differentiation. These genes will be validated by Western blotting and qRT-PCR analyses. To confirm that the genes of interest are involved in the suppression or activation of neuronal differentiation, we will conduct gain- and loss-of-function studies. Follow-up experiments will include chromatin immunoprecipitation followed by sequencing (ChIP-seq) to identify β-catenin binding sites and putative β-catenin binding cofactors and reciprocal co-immunoprecipitation (Co-IP) to validate putative β-catenin interacting factors.

3.2 β-catenin ChIP-seq

We have recently collaborated with Dr. Konrad Basler's lab, a group that has previously performed ChIP-seq on HEK293T cells. They will be applying their experience with β-catenin ChIP-seq to optimize the protocol and perform the bioinformatic analysis. Future experiments will work towards deciphering the precise mechanisms by which β-catenin regulates genes in the absence of TCFs. These mechanisms can be further informed by experiments such as RNA-seq and BioID analyses. RNA-seq can be used to identify differentially expressed genes in WT and QKO mESCs in response to Wnt stimulation. TCF-independent β-catenin-regulated genes identified by this method can be validated by comparing with those identified by ChIP-seq. Furthermore, BioID methodology can be used to identify novel nuclear β-catenin-interacting proteins. BioID is a method that uses a promiscuous biotin ligase (BirA*) to detect proximate and interacting proteins in living cells (Roux et al. 2012). If necessary, putative β-catenin-interacting proteins can be restricted to a developmentally relevant subset. Putative β-catenin binding partners can be reconciled with those identified by *de novo* binding motif analysis of the ChIP-seq data. The top candidates can be validated by reciprocal co-immunoprecipitation (Co-IP) followed by gain- and loss-of-function studies.

3.3 Doxycycline-inducible QKO Cell Lines

Future experiments will aim to knockout the endogenous *CTNNB1* gene in the QKO cell lines with doxycycline-inducible Myc-β-catenin S33A expression. This will allow for the precise doxycycline-regulated control of β-catenin transcription, ranging from a level of nearly zero to very high overexpression levels. Endogenous *CTNNB1*, but not transgenic

CTNNB1, will be knocked out using CRISPRs targeting the 5' untranslated region (UTR) and a 3' splice donor early in the transcript. The CRISPRs have already been designed, generated, and sequence-verified using the design outlined in Figure 16.

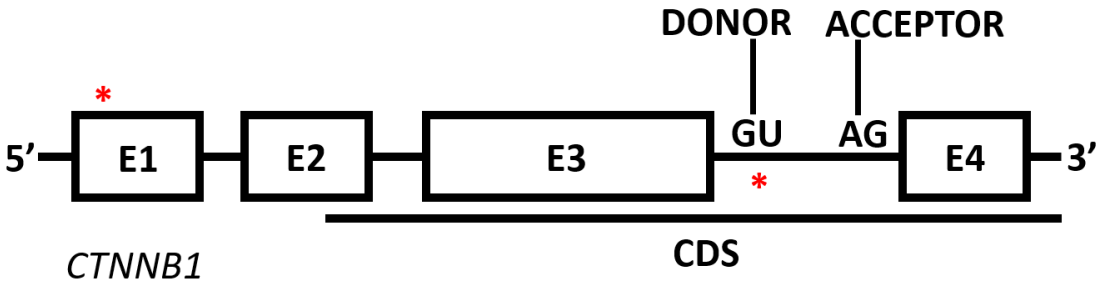

Figure 16. Plan for the CRISPR-mediated knockout of endogenous *CTNNB1*. CRISPRs (denoted by red asterisks) were designed to target the 5' untranslated region and the 3' splicing donor following exon 3.

Upon construction of the cell line, we will determine the impact of β-catenin S33A expression on non-canonical Wnt signalling outputs. We will test non-canonical Wnts in differentiation assays with WT, QKO, and inducible QKO cell lines, with inducible cell lines evaluated at varying levels of β-catenin S33A expression. Differentiation assays will include EB assays and 3-dimensional organoids known as gastruloids, which recapitulate many aspects of early embryonic development (Desbaillets et al. 2000; Simunovic & Brivanlou 2017). EBs and gastuloids will be assessed for their morphology, polarization, and transcript and protein levels of tri-lineage differentiation markers.

4. Concluding Remarks

The findings in this thesis represent a crucial step towards gaining a better understanding of TCF-independent β-catenin regulated signaling mechanisms. Together, our data indicate the presence of a TCF-independent β-catenin regulated neural differentiation blockade in mESCs. Our data also sheds light on potentially problematic methods of ChIP-qPCR data interpretation. Overall, the experiments outlined in this thesis have the potential to unveil new therapeutic targets for the treatment of numerous β-catenin-associated diseases, including cancer, bone-density defects, and type II diabetes (Nusse 2005; Clevers 2006; Macdonald et al. 2009).

References

Aberle, H. et al., 1997. β-catenin is a target for the ubiquitin-proteasome pathway. *The EMBO Journal*, 16(13), pp.3797–3804.

Albrecht, U. et al., 2014. Requirement for Wnt3 in Vertebrate Axis Formation. *Nature Genetics*, 22(4), pp.361–365.

Angers, S. & Moon, R.T., 2009. Proximal events in Wnt signal transduction. *Nature Reviews Molecular Cell Biology*, 10(7), pp.1–10.

Atcha, F.A. et al., 2003. A New Beta-Catenin-dependent Activation Domain in T Cell Factor. *Journal of Biological Chemistry*, 278(18), pp.16169–16175.

Atcha, F.A., Syed, A., Wu, B., Hoverter, N.P., Yokoyama, N.N., Ting, J.H.T., Munguia, J.E., Mangalam, H.J., Marsh, J.L. and Waterman, M.L., 2007. A Unique DNA Binding Domain Converts T-cell Factors into Strong Wnt Effectors. *Molecular and Cellular Biology*, 27(23), pp.8352–8363.

Atlasi, Y. et al., 2013. Wnt Signaling Regulates the Lineage Differentiation Potential of Mouse Embryonic Stem Cells through Tcf3 Down-regulation. *PLoS Genetics*, 9(5).

Aubert, J. et al., 2002. Functional Gene Screening in Embryonic Stem Cells Implicates Wnt Antagonism in Neural Differentiation. *Nature Biotechnology*, 20(12), pp.1240–1245.

Azuara, V. et al., 2006. Chromatin Signatures of Pluripotent Cell Lines. *Nature Cell Biology*, 8(5), pp.532–538.

Baker, J.C., Beddington, R.S.P. & Harland, R.M., 1999. Wnt Signaling in Xenopus Embryos Inhibits Bmp4 Expression and Activates Neural Development. *Genes and*

Development, 13(23), pp.3149–3159.

Baksh, D., Boland, G.M. & Tuan, R.S., 2007. Cross-Talk Between Wnt Signaling Pathways in Human Mesenchymal Stem Cells Leads to Functional Antagonism During Osteogenic Differentiation. *Journal of Cellular Biochemistry*, 101(5), pp.1109–1124.

Batlle-morera, L., Smith, A. & Nichols, J., 2008. Parameters Influencing Derivation of Embryonic Stem Cells From Murine Embryos. *Genesis*, 46(12), pp.758–767.

Becker, K.A. et al., 2006. Self-Renewal of Human Embryonic Stem Cells is Supported by a Shortened G1 Cell Cycle Phase. *Journal of Cellular Physiology*, 209(3), pp.883–893.

Behrens, Jürgen, Jens P. von Kries, Michael Kühl, Laurakay Bruhn, Doris Wedlich, Rudolf Grosschedl, and W.B., 1996. Functional Interaction of Beta-catenin with the Transcription Factor LEF-1. *Nature*, 382(6592), pp.638–642.

Bond, Allison M., Oneil G. Bhalala, and J.A.K., 2013. The Dynamic Role of Bone Morphogenetic Proteins in Neural Stem Cell Fate and Maturation. *Developmental Neurobiology*, 72(7), pp.1068–1084.

Boyer, L.A. et al., 2005. Core Transcriptional Regulatory Circuitry in Human Embryonic Stem Cells. *Cell*, 122(6), pp.947–956.

Carlsson, P., Marian, L.W. & Jones, K.A., 1993. The hLEF / TCF-la HMG protein contains a context-dependent transcriptional activation domain that induces the TCR enhancer in T cells. *Genes and Development*, 7(12), pp.2418–2430.

Castrop, J.A.N., Korinek, V. & Clevers, H., 1996. Extensive Alternative Splicing and

Dual Promoter Usage Generate Tcf-1 Protein Isoforms with Differential Transcription Control Properties. *Molecular and Cellular Biology*, 16(3), pp.745–752.

Chesire, D.R. & Isaacs, W.B., 2002. Ligand-dependent Inhibition of Beta-catenin/TCF Signaling by Androgen Receptor. *Oncogene*, 21(55), pp.8453–8469.

Clevers, H., 2006. Wnt/β-Catenin Signaling in Development and Disease. *Cell*, 127(3), pp.469–480.

Clevers, H. & Nusse, R., 2012. Review Wnt/Beta-Catenin Signaling and Disease.

Singh, S.K. et al., 2004. Identification of human brain tumour initiating cells. *Nature*, 432(7015), pp.396-401.

Daniels, D.L. & Weis, W.I., 2005. β-catenin Directly Displaces Groucho/TLE Repressors from Tcf/Lef in Wnt-mediated Transcription Activation. *Nature Structural & Molecular Biology*, 12(4), pp.364–371.

De, A., 2011. Wnt/Ca2+ Signaling Pathway: A Brief Overview The Non-canonical Wnt Signaling Cascade. *Acta Biochimica et Biophysica Sinica*, 43(10), pp.745–756.

Desbaillets, I. et al., 2000. Gene Manipulation and Integrative Physiology Embryoid bodies: An in vitro Model of Mouse Embryogenesis. *Experimental Physiology*, 85(6), pp.645–651.

Devenport, D., 2014. The Cell Biology of Planar Cell Polarity. *The Journal of Cell Biology*, 207(2), pp.171–180.

Doble, B.W. et al., 2007. Functional Redundancy of GSK-3a and GSK-3β in Wnt/β-Catenin Signaling Shown by Using an Allelic Series of Embryonic Stem Cell Lines.

Developmental Cell, 12(6), pp.957–971.

Gao, C. & Chen, Y., 2010. Dishevelled: The hub of Wnt signaling. *Cellular Signalling*, 22(5), pp.717–727. Available at: http://dx.doi.org/10.1016/j.cellsig.2009.11.021.

Giese, K. et al., 1995. Assembly and function of a TCR enhancer complex is dependent on LEF-l-induced DNA bending and multiple protein-protein interactions. , pp.995–1008.

Ginis, I. et al., 2004. Differences between Human and Mouse Embryonic Stem Cells. *Developmental Biology*, 269(2), pp.360–380.

Gordeeva, O.F. & Nikonova, T.M., 2013. Development of Experimental Tumors Formed by Mouse and Human Embryonic Stem and Teratocarcinoma Cells After Subcutaneous and Intraperitoneal Transplantations Into Immunodeficient and Immunocompetent Mice. *Cell Transplantation*, 22(10), pp.1901–1914.

Grumolato, L. et al., 2010. Canonical and Noncanonical Wnts use a Common Mechanism to Activate Completely Unrelated Coreceptors. *Genes and Development*, 24(22), pp.2517–2530.

Habas, R., Dawid, I.B. & He, X., 2003. Coactivation of Rac and Rho by Wnt/Frizzled Signaling is Required for Vertebrate Gastrulation. *Genes and Development*, 17(2), pp.295–309.

Haegele, L. et al., 2003. Wnt Signalling Inhibits Neural Differentiation of Embryonic Stem Cells by Controlling Bone Morphogenetic Protein Expression. *Molecular and Cellular Neuroscience*, 24(3), pp.696–708.

Haring, M. et al., 2007. Chromatin Immunoprecipitation: Optimization, Quantitative

Analysis and Data Normalization. *Plant Methods*, 3(1), pp.1–16.

Hartsock, A. & Nelson, W.J., 2008. Adherens and tight junctions : Structure , function and connections to the actin cytoskeleton. *Biochimica et Biophysica Acta (BBA)-Biomembranes*, 1778, pp.660–669.

Hikasa, H., Ezan, J., Itoh, K., Li, X., Klymkowsky, M. W., & Sokol, S.Y., 2011. Regulation of TCF3 by Wnt-dependent Phosphorylation during Vertebrate Axis Specification. *Developmental Cell*, 19(4), pp.521–532.

Hoffmeyer, K. et al., 2017. Trimethylation and Acetylation of β-Catenin at Lysine 49 Represent Key Elements in ESC Report Trimethylation and Acetylation of β-Catenin at Lysine 49 Represent Key Elements in ESC Pluripotency. *Cell Reports*, 18(12), pp.2815–2824.

Houbaviy, H.B., Murray, M.F. & Sharp, P.A., 2003. Embryonic Stem Cell-Specific MicroRNAs. *Developmental Cell*, 5(2), pp.351–358.

Hsu, W., Zeng, L. & Costantini, F., 1999. Identification of a Domain of Axin That Binds to the Serine / Threonine Protein Phosphatase 2A and a Self-binding Domain. *Journal of Biological Chemistry*, 274(6), pp.3439–3445.

Huber, A.H., Nelson, W.J. & Weis, W.I., 1997. Three-Dimensional Structure of the Armadillo Repeat Region of Beta-Catenin. *Cell*, 90, pp.871–882.

Huelsken, J. et al., 2000. Requirement for Beta-Catenin in Anterior-Posterior Axis Formation in Mice. *Journal of Cell Biology*, 148(3), pp.567–578.

Johnson, M.H., 1981. The Foundation of Two Distinct within the Mouse Morula. *Cell*, 24(1), pp.71–80.

Kadam, S., Emerson, B.M. & Jolla, L., 2003. Transcriptional Specificity of Human SWI / SNF BRG1 and BRM Chromatin Remodeling Complexes. *Molecular Cell*, 11, pp.377–389.

Kaufman, M.J.E.& M.H., 1981. Establishment in Culture of Pluripotential Cells from Mouse Embryos. *Nature*, 292(5819), pp.154–156.

Kawano, Y. & Kypta, R., 2003a. Secreted Antagonists of the Wnt Signalling Pathway. *Journal of Cell Science*, 116(13), pp.2627–2634.

Kelly, K.F. et al., 2011. β-Catenin Enhances Oct-4 Activity and Reinforces Pluripotency through a TCF-Independent Mechanism. *Stem Cell*, 8(2), pp.214–227.

Kelly, O.G., Pinson, K.I. & Skarnes, W.C., 2004. The Wnt co-receptors Lrp5 and Lrp6 are Essential for Gastrulation in Mice. *Development*, 131(12), pp.2803–2815.

Kielman, M.F. et al., 2002. Apc modulates embryonic stem-cell differentiation by controlling the dosage of β-catenin signaling. *Nature Genetics*, 32(4), pp.594-605.

Klingel, S. et al., 2012. Subfunctionalization and neofunctionalization of vertebrate Lef / Tcf transcription factors. *Developmental Biology*, 368(1), pp.44–53.

Kramps, T. et al., 2002. Wnt/Wingless Signaling Requires BCL9/Legless-Mediated Recruitment of Pygopus to the Nuclear Beta-Catenin-TCF Complex. *Cell*, 109(1), pp.47–60.

Kuwabara, T. et al., 2009. Wnt-mediated Activation of NeuroD1 and Retro-elements during Adult Neurogenesis. *Nature Neuroscience*, 12(9), pp.1097–1105.

Lee, J. & Lee, M.C., 2014. Generation of Cancerous Neural Stem Cells Forming Glial Tumor by Oncogenic Stimulation. *Stem Cells Reviews and Reports*, 8(2), pp.532–

545.

Liu, C. et al., 2002. Control of Beta-Catenin Phosphorylation / Degradation by a Dual-Kinase Mechanism. *Cell*, 108, pp.837–847.

Lyashenko, N., Winter, M., Migliorini, D., Biechele, T., Moon, R.T. and Hartmann, C., 2012. Differential Requirement for the Dual Functions of β-catenin in Embryonic Stem Cell Self-Renewal and Germ Layer Formation. *Nature Cell Biology*, 13(7), pp.753–761.

Macdonald, B.T., Tamai, K. & He, X., 2009. Wnt/Beta-Catenin Signaling: Components , Mechanisms , and Diseases. *Developmental Cell*, 17(1), pp.9–26.

Marin, O. et al., 2003. A noncanonical sequence phosphorylated by casein kinase 1 in Beta-catenin may play a role in casein kinase 1 targeting of important signaling proteins. *Proceedings of the National Academy of Science*, 100(18), pp.10193-10200.

Martello, G. et al., 2012. Esrrb Is a Pivotal Target of the Gsk3/Tcf3 Axis Regulating Embryonic Stem Cell Self-Renewal. *Cell Stem Cell*, 11(4), pp.491–504.

Martin, G.R., 1981. Isolation of a Pluripotent Cell Line from Early Mouse Embryos Cultured in Medium Conditioned by Teratocarcinoma Stem Cells. *Proceedings of the National Academy of Sciences of the United States of America*, 78(12), pp.7634–7638.

Martinez, S. et al., 2015. The PTK7 and ROR2 Protein Receptors Interact in the Vertebrate WNT / Planar Cell Polarity (PCP) Pathway. *Journal of Biological Chemistry*, 290(51), pp.30562–30572.

Mcculloch, E.A. & Till, J.E., 1963. Cytological Demonstration of the Clonal Nature of

Spleen Colonies Derived from Transplanted Mouse Marrow C ells. *Nature*, 197(4866), pp.452–454.

Meijer, L. et al., 2004. Maintenance of Pluripotency in Human and Mouse Embryonic Stem Cells through Activation of Wnt Signaling by a Pharmacological GSK-3-Specific Inhibitor. *Nature Medicine*, 10(1), pp.55–63.

Molenaar, M. et al., 1996. XTcf-3 Transcription Factor Mediates Beta-Catenin-Induced Axis Formation in Xenopus Embryos. *Cell*, 86(3), pp.391–399.

Muñoz-sanjuán, I. & Brivanlou, A.H., 2002. Neural Induction, the Default Model and Embryonic Stem Cells. *Nature Reviews Neuroscience*, 3(4), pp.1–10.

Nagy, A. et al., 1993. Derivation of Completely Cell Culture-derived Mice from Early-passage Embryonic Stem Cells. *Proceedings of the National Academy of Sciences of the United States of America*, 90(18), pp.8424–8428.

Naylor, S. et al., 2000. Retroviral expression of Wnt-1 and Wnt-7b produces different effects in mouse mammary epithelium. *J Cell Sci*, 2138, pp.2129–2138.

Nusse, R., 2005. Wnt Signaling in Disease and in Development. *Cell Research*, 15(1), pp.28–32.

Nusse, R. & Varmust, H.E., 1992. Wnt Genes. *Cell*, 69(7), pp.1073–1087.

Nüsslein-Volhard, C., Wieschaus, E. and Kluding, H., 1984. Mutations Affecting the Pattern of the Larval Cuticle in Drosophila Melanogaster. *Wilhelm Roux's Archives of Developmental Biology*, 193(5), pp.283–295.

Ohtsuka, S., Nakai-futatsugi, Y. & Niwa, H., 2015. LIF Signal in Mouse Embryonic Stem Cells. *JAK-STAT*, 4(2), pp.1–19.

Okita, K., Ichisaka, T. & Yamanaka, S., 2007. Generation of Germline-Competent Induced Pluripotent Stem Cells. *Nature*, 448(7151), pp.313–318.

Orford, K. et al., 1997. regulated Ubiquitination and Degradation of -Catenin *. , pp.24735–24739.

Otero, J.J. et al., 2004. β-Catenin Signaling is Required for Neural Differentiation of Embryonic Stem Cells. *Development*, 131(15), pp.3545–3557.

Przyborski, S.A. et al., 2004. Human Embryonal Carcinoma Stem Cells: Models of Embryonic Development in Humans. *Stem Cells and Development*, 13(4).

Qi, X. et al., 2004. BMP4 supports self-renewal of embryonic stem cells by inhibiting mitogen-activated protein kinase pathways. *Proceedings of the National Academy of Sciences of the United States of America*, 101(16), pp.6027–6032.

Reya, T. et al., 2000. Wnt Signaling Regulates B Lymphocyte Proliferation through a LEF-1 Dependent Mechanism. *Immunity*, 13(1), pp.15–24.

Roux, K.J. et al., 2012. A Promiscuous Biotin Ligase Fusion Protein Identifies Proximal and Interacting Proteins in Mammalian Cells. *The Journal of Cell Biology*, 196(6), pp.801–810.

Schweizer, L. et al., 2008. The Androgen Receptor can Signal through Wnt/β-Catenin in Prostate Cancer Cells as an Adaptation Mechanism to Castration Levels of Androgens. *BMC Cell Biology*, 9(1), pp.1–15.

Shi, Y. & Massague, J., 2003. Mechanisms of TGF-β Signaling from Cell Membrane to the Nucleus. *Cell*, 113(6), pp.685–700.

Shimizu, T. et al., 2008. Stabilized Beta-Catenin Functions through TCF/LEF Proteins

and the Notch/RBP-J Complex To Promote Proliferation and Suppress Differentiation of Neural Precursor Cells. *Molecular and Cellular Biology*, 28(24), pp.7427–7441.

Shitashige, M., Satow, R., Honda, K., Ono, M., Hirohashi, S. and Yamada, T., 2008. Regulation of Wnt Signaling by the Nuclear Pore Complex. *Gastroenterology*, 134(7), pp.1961–1971.

Shy, B.R. et al., 2013. Regulation of Tcf7l1 DNA Binding and Protein Stability as Principal Mechanisms of Wnt/β-catenin Signaling. *Cell Reports*, 4(1), pp.1–9.

Simunovic, M. & Brivanlou, A.H., 2017. Embryoids , Organoids and Gastruloids: New Approaches to Understanding Embryogenesis. *Development*, 39(3), pp.976–985.

Slawny, N.A. & Shea, K.S.O., 2011. Dynamic Changes in Wnt signaling are Required for Neuronal Differentiation of Mouse Embryonic Stem Cells. *Molecular and Cellular Neuroscience*, 48(3), pp.205–216.

Stamos, J.L. & Weis, W.I., 2013. The Beta-Catenin Destruction Complex. *Science*, pp.1–16.

Sutherland, C., 2011. What Are the Bona Fide GSK3 Substrates ? *International Journal of Alzheimer's Disease*, 2011, pp.1–23.

Takao, Y., Yokota, T. & Koide, H., 2007. β-Catenin Up-regulates Nanog Expression through Interaction with Oct-3/4 in Embryonic Stem Cells. *Biochemical and Biophysical Research Communications*, 353(3), pp.699–705.

Takao, Y., Yokota, T. & Koide, H., 2007. Beta-catenin Upregulates Nanog Expression Through Interaction with Oct-3/4 in Embryonic Stem Cells. *Biochemical and*

Biophysical Research Communications, 353(3), pp.669–705.

Tamai, K. et al., 2004. A Mechanism for Wnt Coreceptor Activation. *Molecular Cell*, 13(1), pp.149–156.

Taurog, R. E., Jakubowski, H., & Matthews, R.G., 2006. Random Sequential Binding of Substrates in Cobalamin-Independent Methionine Synthase. *Biochemistry*, 45(16), pp.5083–5091.

Tropepe, V. et al., 2001. Direct Neural Fate Specification from Embryonic Stem Cells : A Primitive Mammalian Neural Stem Cell Stage Acquired through a Default Mechanism. *Neuron*, 30(1), pp.65–78.

Ueno, N. & Greene, N.D.E., 2003. Planar Cell Polarity Genes and Neural Tube Closure. *Birth Defects Research*, 69(4), pp.318–324.

Vacik, T. et al., 2011. Dominant-negative Isoforms of Tcf/Lef Proteins in Development and Disease. *Cell Cycle*, 10(24), pp.9–11.

Valenta, T., Hausmann, G. & Basler, K., 2012a. The many faces and functions of b -catenin. , 31(12), pp.2714–2736.

Valenta, T., Hausmann, G. & Basler, K., 2012b. The Many Faces and Functions of Beta-catenin. *The EMBO Journal*, 31(12), pp.2714–2736.

Wang, R.N. et al., 2014. Bone Morphogenetic Protein (BMP) Signaling in Development and Human Diseases. *Genes & Diseases*, 23(4), pp.87–105.

Wang, Y. & Nathans, J., 2007. Tissue/Planar Cell Polarity in Vertebrates: New Insights and New Questions. *Development*, 134(4), pp.647–658.

Weise, A. et al., 2010. Alternative splicing of Tcf7l2 transcripts generates protein variants

with differential promoter-binding and transcriptional activation properties at Wnt/Beta-catenin targets. *Nucleic Acids Research*, 38(6), pp.1964–1981.

Wen, S., Li, H. & Liu, J., 2009. Dynamic Signaling for Neural Stem Cell Fate Determination. *Cell Adhesion and Migration*, 3(1), pp.107–117.

Wilson, S. et al., 2015. Neural induction: Toward a Unifying Mechanism. *Nature Neuroscience*, 4, pp.1161–1168.

Wilson, P. A., & Hemmati-Brivanlou, A., 1995. Induction of Epidermis and Inhibition of Neural Fate by Bmp-4. *Nature*, 376(6538), pp.331–333.

Wray, J. et al., 2011. Inhibition of Glycogen Synthase Kinase-3 Alleviates Tcf3 Repression of the Pluripotency Network and Increases Embryonic Stem Cell Resistance to Differentiation. *Nature Cell Biology*, 13(7), pp.838–845.

Wu, J., & Mlodzik, M., 2008. The Frizzled Extracellular Domain Is a Ligand for Van Gogh/Stbm during Vertebrate Gastrulation. *Developmental Biology*, 15(3), pp.462–469.

Yi, F. et al., 2012. Opposing effects of Tcf3 and Tcf1 control Wnt stimulation of embryonic stem cell self-renewal. *Nature Cell Biology*, 13(7), pp.762–770.

Ying, L. et al., 2015. OCT4 Coordinates with WNT Signaling to Pre-pattern Chromatin at the SOX17 Locus during Human ES Cell Differentiation into Definitive Endoderm. *Stem Cell Reports*, 5(4), pp.490–498.

Ying, Q. et al., 2003. BMP Induction of Id Proteins Suppresses Differentiation and Sustains Embryonic Stem Cell Self-Renewal in Collaboration with STAT3. *Cell*, 115(3), pp.281–292.

Ying, Q. et al., 2008. The Ground State of Embryonic Stem Cell Self-renewal. *Nature*, 453(7194), pp.519–524.

Yokoya, F. et al., 1999. Beta-Catenin can be Transported into the Nucleus in a Ran-unassisted Manner. *Molecular Biology of the Cell*, 10(4), pp.1119–1131.

Zeng, P. et al., 2006. In Vivo Dual Cross-linking for Identification of Indirect DNA-associated Proteins by Chromatin Immunoprecipitation. *Biotechniques*, 41(6), pp.2–4.

Zhang, X., Peterson, K. A., Liu, X. S., McMahon, A. P., & Ohba, S., 2013. Gene Regulatory Networks Mediating Canonical Wnt Signal-Directed Control of Pluripotency and Differentiation in Embryo Stem Cells. *Stem Cells*, 31(12), pp.2667–2679.